Advancing Peripheral Nerve Interfaces in a Large Animal Model

Rettore Andreis, Felipe

DOI (link to publication from Publisher):
10.54337/aau478976327

Publication date:
2022

Document Version
Publisher's PDF, also known as Version of record

ADVANCING PERIPHERAL NERVE INTERFACES IN A LARGE ANIMAL MODEL

BY
FELIPE RETTORE ANDREIS

DISSERTATION SUBMITTED 2022

AALBORG UNIVERSITY
DENMARK

ADVANCING PERIPHERAL NERVE INTERFACES IN A LARGE ANIMAL MODEL

by

Felipe Rettore Andreis

AALBORG UNIVERSITY
DENMARK

Dissertation submitted

2022

Dissertation submitted:	08th April 2022
PhD supervisor:	Associate Prof. Thomas Gomes Nørgaard dos Santos Nielsen Aalborg University
Assistant PhD supervisor:	PhD co-supervisor: Prof. Winnie Jensen Aalborg University
PhD committee:	Associate Professor Jacob Melgaard Aalborg University, Denmark
	Associate Professor Paul Yoo University of Toronto, Canada
	Professor Peter Veltink University of Twente, The Netherlands
PhD Series:	Faculty of Medicine, Aalborg University
Department:	Department of Health Science and Technology

ISSN (online): 2246-1302
ISBN (online): 978-87-7573-916-5

Published by:
Aalborg University Press
Kroghstræde 3
DK – 9220 Aalborg Ø
Phone: +45 99407140
aauf@forlag.aau.dk
forlag.aau.dk

Printed in Denmark by Stibo Complete, 2022

CV

Felipe holds a B.Sc. in Electrical Engineering from the University of Passo Fundo (Brazil) and an M.Sc. in Electrical Engineering with a focus on Biomedical Engineering from the Federal University of Santa Catarina (Brazil). He enrolled at Aalborg University as a Marie Skłodowska-Curie FRESCO PhD fellow under the supervision of Thomas Gomes Nørgaard dos Santos Nielsen and co-supervision of Winnie Jensen. He is part of the Neural Engineering and Neurophysiology group and part of the Center for Neuroplasticity and Pain (CNAP), both at the Department of Health Science and Technology. Felipe's PhD project was supported by the Horizon 2020 research and innovation programme (Grant no. 754465) and the Danish National Research Foundation (DNRF121).

ENGLISH SUMMARY

Implantable neural interfaces have been used for several decades in research and clinical applications to modulate the autonomic nervous system and restore amputees' motor and sensory function. Several electrode designs exist to achieve such a goal. Still, to date, the most widely adopted interface is the extraneural cuff electrode, with its main advantages of simple surgical implantation and extended chronic viability. However, given the intrinsic noisy environment and the small selectivity of extraneural cuffs, its recording capabilities are limited, resulting in most of its applications as "open-loop" systems. To improve the recording selectivity of extraneural cuffs, a method using multi-electrode configurations, which, combined with a simple delay-and-add operator, makes it possible to infer fibre type and direction of propagation, has been suggested. In addition, the simplicity of the system enables its use for "closed-loop" applications.

Another factor limiting the improvement of peripheral nerve interfaces is the gap between the peripheral nerve structure of small animal models and humans. To name a few of the differences, the smaller nerves and simpler fascicular structures can create significant differences in stimulation thresholds when moving from research to clinical applications. There is a growing body of literature suggesting that the peripheral nervous system of pigs may provide a better translational model than the commonly used rodents. However, our knowledge of the peripheral nervous system of pigs, especially the somatic nervous system, is still limited.

Therefore, this thesis aimed to advance peripheral nerve interfaces in a large animal model (i.e., the pig). Three studies were designed to achieve this goal. In Study I, the morphological features of the ulnar nerve were explored with a histological assessment. This study aimed at answering the following question: is the neuroanatomy of the ulnar nerve in pigs more comparable to humans than rodents? Study II aimed at characterising the excitability properties of the ulnar nerve in pigs through a wide range of electrical stimulation parameters while, at the same time, recording the neural activity with a multiple-electrode cuff. Finally, Study III investigated several algorithms for extracting information from linear electrode arrays. While the delay-and-add operator has been traditionally used in electroneurography, different approaches have been adopted for similar problems in other research areas, which led us to assess and compare the performance of each suitable algorithm with simulated and in vivo data.

In summary, the results from study I show the feasibility of using a multiple-electrode cuff to distinguish fibre population and provide data for researchers aiming to use the ulnar nerve in pigs as a model for probing the neural circuitry. Study II provides a detailed analysis of the ulnar nerve morphology in pigs. It shows how the pig can be a suitable translational model for peripheral nervous system studies. Finally, study III

evaluates several algorithms for extracting information from multiple-electrode cuffs and discusses the advantages and drawbacks of each. This work contributes to the advancement of peripheral nerve interfaces by exploring an ulnar nerve model in a porcine, representing a step forward in using large animal models for peripheral nerve interface research.

DANSK RESUME

Implanterbare neurale grænseflader er blevet brugt gennem flere årtier i forskning og kliniske applikationer til at modulere det autonome nervesystem og genoprette amputeredes motoriske og sensoriske funktion. Der findes idag adskillige elektrodedesigns til formålet. Til dato, er den mest udbredte nervegrænseflade stadig den ekstraneurale manchetelektrode. Dens vigtigste fordel er at være enkel at implantere kirurgisk i kroppen samt, at den har høj kronisk levedygtighed. Men på grund af at elektroden er placeret i kroppen tæt på andre fysiologisk støjende signaler, og den har en lav selektivitet, er dens evner til at optage det perifere nervesignal begrænsede. Det resulterer i at de fleste applikationer, hvor elektroden indgår i, er "open-loop" systemer. For at forbedre kvaliteten af optagelserne er det derfor tidligere foreslået at multi-elektrode-konfigurationer, som kombineret med en enkel 'delay-and-add' gør det muligt at udlede information om hvilken fibertype og hvilken retning som aktionspotentialet bevæger sig i. Det baner vejen for at få bedre signaler og dermed facilitere anvendelsen af "closed-loop" applikationer.

En anden faktor, der begrænser forbedringen af perifere nervegrænseflader, er forskellen mellem den perifere nervestruktur af små dyremodeller og mennesker. For eksempel kan mere simpel fasikulær struktur i små nerver forårsage markante forskelle i stimuleringstærskler, der har en betydning, når man skal overføre forskning i dyr til kliniske applikationer. Der er en del litteratur der peger på at det perifere nervesystem i grise er en bedre translationel model end almindelig anvendte gnavere. Vores viden om det perifere nervesystem hos grise, især det somatiske nervesystem, er dog stadig begrænset.

Derfor var formålet med denne Ph.D-afhandling at forbedre perifere nervegrænseflader i en stor dyremodel (dvs. i grise). Tre studier blev designet til at nå dette mål. I Studie I blev ulnar nervens morfologi karakteriseret via histologiske undersøgelser. Studiet leverede en detaljeret undersøgelse af neuroanatomien af ulnarnerven hos grise sammenlignet med mennesker og gnavere. Formålet med Studie II var at karakterisere excitabilitets-egenskaberne af ulnarnerven hos grise ved at applicere en bred vifte af elektriske stimuleringsparametre, mens den neurale aktivitet samtidigt blev optaget med en flerelektrodemanchet. Resultaterne fra Studie II viste at en flerelektrodemanchet kunne anvendes til at detektere fiberpopulationer. Til sidst var målet med Studie III at sammenligne algoritmer til at udtrække information fra lineære elektrodearrays. 'Delay-and-add' algoritmen er traditionelt blevet brugt indenfor elektroneurografi, men andre algoritmer er blevet anvendt på lignende problemer indenfor andre forskningsområder, hvilket førte os til at vurdere og sammenligne ydeevnen af hver algoritme med simulerede og in vivo-data.

Denne Ph.D afhandling har bidraget til at forbedre perifere nervegrænseflader ved at undersøge en ulnar nervemodel i grise, hvilke et er skridt fremad mod at bruge store dyremodeller i til forksning i perferiere nervegrænseflader.

ACKNOWLEDGEMENTS

I would like to start the acknowledgements section by thanking my PhD supervisor Thomas Gomes Nørgaard dos Santos Nielsen, who has helped me tremendously and has always inspired me with his in-depth understanding of the topic and critical view of science. More than a supervisor, Thomas has become a good friend of mine. Secondly, I would like to thank my "second" supervisor, Winnie Jensen, for all her support and patience with me during this period. Winnie has always been a positive person that made the work environment truly enjoyable, even in the tensest moments in the lab when things were not going as planned. Now, to both my supervisors, I would like to say that it has been an absolute privilege to work under your guidance, and I will always be grateful for the opportunity you gave me.

I would like to thank my colleague in the experiments, Taha, who always had a positive attitude even in unfavourable scenarios and from whom I have learned enormously, especially in overcoming problems. My thanks extend to Suzan for always being a good friend and office mate and providing a critical perspective about my work, which I genuinely appreciate. I would like to thank Ben for always being helpful and providing significant criticism and insights. Lastly, I would like to thank the lab animal technicians, especially Torben, for his consistent assistance throughout the experiments.

I would also like to thank my colleagues at CNAP and the Department of Health Science and Technology for the fruitful discussions and support. A special thanks go to Sebastian Hjorth, Lea Tøttrup, and Line Lykholt for being wonderful friends and PhD colleagues.

I would like to thank my wife Fernanda for all her support during this period, in which we have been far from each other half of the time, and, despite that, she has always been encouraging me to pursue what I love to do. Also, thanks for helping me with the graphical illustrations. Finally, I would like to thank my parents and brother, who, even though I have not seen them in three years, have always been supportive of my choice to move across the Atlantic.

TABLE OF CONTENTS

TABLE OF FIGURES

CHAPTER 1. INTRODUCTION

Using external devices to interface with the peripheral nervous system (PNS) has a long history, starting when Luigi Galvani (1737 – 1798) used electrical stimulation to produce a movement in the frog's leg in 1771. Current applications encompass the treatment of several diseases, including but not limited to bladder dysfunction [1], therapy-resistant depression [2] and chronic migraine [3]. Besides the treatment of pathologies, interfaces with the PNS have also been used to control artificial limb prostheses to restore sensory and motor function in patients with partial or total limb amputation [4].

Several peripheral nerve interfaces have been developed to stimulate or record from the peripheral nervous system [5], and despite encouraging results, especially of neural stimulation for motor control, significant limitations are still present. In the case of limb prostheses, one of the main drawbacks has been the inability of the prosthesis to produce natural feedback, resulting in decreased user acceptability and confidence in the prosthesis [6]. In bioelectronic medicine, most systems depend on open-loop stimulation methods, where the stimulation parameters are preprogrammed [7], [8]. Therefore, open-loop systems do not account for alterations in the patient's physiology following the implant or changes in the bioelectric medium, which can degrade the interface performance so that preprogrammed stimulation parameters are no longer effective.

Another area where PNIs are used is basic neuroscience research, where electrical stimulation is used to probe the central nervous system. For instance, experiments in pain research have commonly adopted electrical stimulation to evoke painful sensations and then investigate the cortical responses [9], [10]. In humans, that is achieved by simply asking subjects to rate their pain state. However, the same cannot be done to animals. Therefore, compound action potentials need to be recorded and fibre types classified to ensure a proper stimulation level. Ideally, a closed-loop system would be used to adjust the necessary stimulation intensities for exciting specific fibre groups based on the recording signals.

The limitations presented, both for bioelectronic medicine, limb prostheses, and neuroscience, result from the challenging task of decoding information from the PNS. Two key factors can be used to highlight why that is the case. The first is the inherently poor signal-to-noise ratio of the electroneurographic signal, which poses difficulties in distinguishing the neural signal from external noise sources [11]. The second, and not least important, is that the structure of the PNS is rich in information, containing thousands of nerve fibres with specific functions collected into one or many fascicles [12]. Therefore, the ideal interface should be able to stimulate/record selectively from distinct fibre classes or distinct fascicles within a nerve while at the same time being chronically safe and stable.

The advancement of peripheral nerve interfaces requires thoughtful consideration for selecting an appropriate pre-clinical model, as the morphological characteristics of the nerve have a significant influence on the electrode design and stimulation parameters [13]. An animal model that resembles the human analogue may facilitate translational knowledge from basic research to clinical applications. Recent evidence suggests that porcine peripheral nerves are more comparable to humans in size, fascicular structure, and tissue type [14], [15]. Nevertheless, most studies investigating the peripheral nerves of pigs are focused on the autonomic nerves, and the knowledge of the morphometry of somatic nerves of large animals is still limited.

Therefore, the focus of this thesis was to provide information that is essential for developing novel interfaces and realistic computational models of the peripheral nervous system of large animals and, in addition, to investigate alternative ways of extracting information from extraneural interfaces.

CHAPTER 2. STATE OF THE ART

2.1. PERIPHERAL NERVES

2.1.1. NERVE STRUCTURE

The PNS is connected bidirectionally with the central nervous system (CNS) through bundles of axons extending from the CNS to the target organs. The PNS is further divided into the somatic and autonomic nervous systems. The somatic nervous system is responsible for controlling voluntary muscle movement and providing sensory information about the environment outside the body. In contrast, the autonomic nervous system regulates bodily functions of internal organs (e.g., heart and respiratory rate, bladder activity) [4].

Peripheral nerves consist of individual nerve fibres surrounded by an outer endoneurial sheath. The nerve fibres are then arranged in bundles of fascicles, which in turn, are grouped by a layer of connective tissue called the perineurium. The perineurium is the main component that provides elasticity and tensile strength to the nerve. Finally, the fascicles are packed by the epineurium, the outermost sheath of the nerve [12]. An illustration of the peripheral nerve structure is displayed in Figure 2.1.

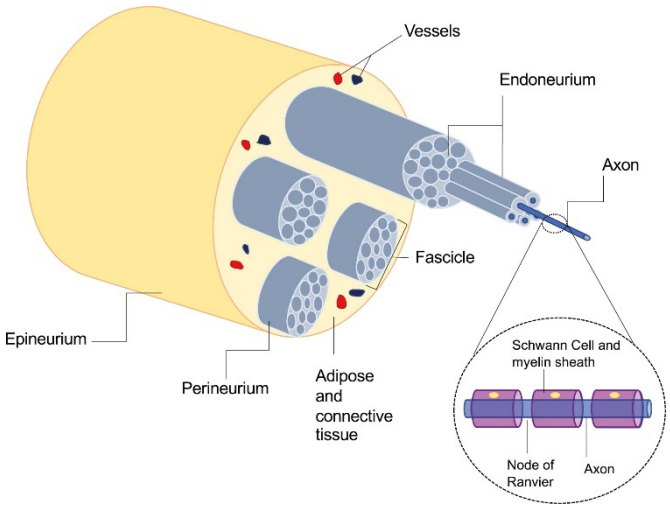

Figure 2.1. Illustration of the peripheral nerve structure. Reprinted from Journal of Orthopaedics, Volume 22, Rodriguez-Fontan et al., Tobacco use and neurogenesis: A theoretical review of pathophysiological mechanisms affecting the outcome of peripheral nerve regeneration, Pages 59-63, Copyright (2022), with permission from Elsevier.

The internal topography of peripheral nerves is highly variable and depends on the specific nerve, anatomical location, and species. Several features are used to characterise a nerve. For instance, by fascicles, which are categorised as monofascicular, oligofascicular, or polyfascicular [16]. Interestingly, the fascicular number can vary from 1 to more than 100 and does not only differ between different nerves but also can have significant variations within the same nerve at different points [16]. The number of fibres can also significantly change in segments of the same nerve a few millimetres apart [12]. For example, the number of fibres of the Wistar rat radial nerve ranged from 1372 to 397 in proximal and distal sections, respectively [17]. Different species also display a significant difference in the number of fibres within a nerve (e.g., a study investigating the number of fibres in the cervical vagus nerve of mice and humans reported 1426 fibres for the first and 51288 for the latter) [15].

2.1.2. NERVE CELL STRUCTURE AND FUNCTION

The neuron is the functional part of the PNS and the CNS. They are specialised in transmitting messages from one part of the body to another, and they can have a range of sizes and shapes; however, most of them are formed by four parts: (i) axon terminals, (ii) an axon, (iii) dendrites, and (iv) a cell body [18].

Neurons are excitable cells polarised at the resting state, with the inside of the cell negatively charged with respect to the outside. This state is termed resting membrane potential, and at this state, the cell will typically have an amplitude of -70 mV. Many stimuli can generate transient changes in the membrane potential, therefore exciting neurons to become active and initiate local depolarisation, which, if strong enough, can generate an action potential (AP). The APs are rapid alterations in the membrane potential (usually from -70 mV to +30 mV) and are the mechanism used by the nervous system to communicate over long distances [19]. APs have four essential properties for neuronal signalling: (i) they have a threshold voltage required for the AP initiation, (ii) APs have an *all-or-none* response, meaning that a large depolarising current results in the same AP as an even larger depolarising current, (iii) the AP amplitude does not decrease with distance, and (iv) the AP is followed by a refractory period [20].

2.1.3. FUNCTIONAL CLASSIFICATION OF NERVE FIBRES

The nerve fibres are classified according to the direction of propagation of nerve impulses relative to the CNS. Nerves that convey impulses *to* the CNS from sensory receptors are named *afferent* ("to go toward"). In contrast, *efferent* nerve fibres carry impulses *from* the CNS to effector organs, glands, and muscles [21]. The seminal work of Gasser and Erlanger [22], [23] has led to a classification of nerve fibres based on their diameter and degree of myelination, which the authors showed to be positively correlated to the conduction velocity and associated with specific functions.

Their work resulted in the 'textbook' classification of fibre types, as shown in Table 2.1 [24].

Table 2.1. The traditional classification of fibre types in mixed nerve bundles [24].

Type of fibre	**Class**	**Radius (µm)**	**MCV[1] (ms^{-1})**	**General function**
Aα	Myelinated	12-20	70-120	Proprioception, somatomotor
Aβ	Myelinated	5-12	30-70	Touch, pressure
Aγ	Myelinated	3-6	15-30	Motor for muscle spindles
Aδ	Thinly myelinated	2-5	12-30	Pain, cold, touch
B	Thinly myelinated	<3	3-15	Pregnanglionic autonomic
C	Unmyelinated	0.2-2	0.5-2	Pain, temperature, mechanoreception

[1]Mean Conduction Velocity

Measuring fibre diameter would require obtaining cross-sections of nerves and performing specialised histological procedures. Thus, because of the proportional relationship between fibre diameter and conduction velocity, one can indirectly assess peripheral nerve state with electrophysiological techniques by measuring nerve conduction velocity [25]. The nerve conduction velocity has been a valuable metric for diagnosis, prognosis, and description of PNS disorders [26] and is also essential for the development of closed-loop interfaces [27], [28].

2.2. IMPLANTABLE NEURAL INTERFACES

2.2.1. APPLICATIONS

Interfacing with the peripheral somatic or autonomic nervous system is an attractive tool to monitor and modulate neural activity. The first clinical application with peripheral nerve interfaces (PNIs) was seen in the late 1960s to control hemiplegic gait [29], urinary incontinence [30] and electrophrenic respiration [31]. Nerve interfaces, like the PNS, can exchange information with the CNS bidirectionally. In the two aforementioned examples, the interface was used to excite neural tissue, particularly the phrenic and pudendal nerves. While electrical stimulation is

commonly used to restore impaired function via PNIs, recording the nervous system's activity can determine the state of an organ and provide feedback or command to control a prosthetic device [32].

The applications of PNIs can be broadly divided into two categories: bioelectronic medicine and functional electrical stimulation. Bioelectronic medicine concerns modulating the ANS to compensate for dysfunctional circuits leading to disease to achieve therapeutic effects. Ideally, this is done in a closed-loop manner, where recording and decoding of the neural signal are used to detect dysfunctional activity, activating external devices to modulate the flawed system. Currently, there are numerous FDA-approved clinical studies investigating the prospective of bioelectronic medicine systems; these include, but are not limited to, treatment of obesity [33], chronic migraine [3], epilepsy [34] and treatment-resistant depression [35].

While bioelectronic medicines focus on the autonomic nervous system, functional electrical stimulation revolves around using electrical stimulation to restore motor function in paralysed or paretic muscles. Examples of successful applications of functional electrical stimulation include correction of footdrop [36] and providing sensory feedback for amputee patients with limb prostheses [6].

2.2.2. PERIPHERAL NERVOUS SYSTEM ELECTRODES

Ideally, a PNI should be able to extract and decode the information from every neuron within a nerve and be chronically safe. As the number of fibres in a nerve can be tens of thousands, this is currently an unrealised task. Therefore, a wide range of interfaces was developed to approximate the ideal model, each with its advantages and shortcomings [8], [37].

PNIs are usually defined by their level of invasiveness; therefore, the more invasive the interface, the closer it is to the nerve fibres, resulting in a higher spatial selectivity. A high selectivity comes with the cost of reducing safety and chronic viability. This effect is known as the invasiveness – selectivity trade-off. The current range of nerve interfaces can be classified into three broad categories: extraneural (on the nerve), intraneural (within the nerve) interfaces, and regenerative interfaces [38]. An illustration of the location of current interfaces in the trade-off curve is shown in Figure 2.2.

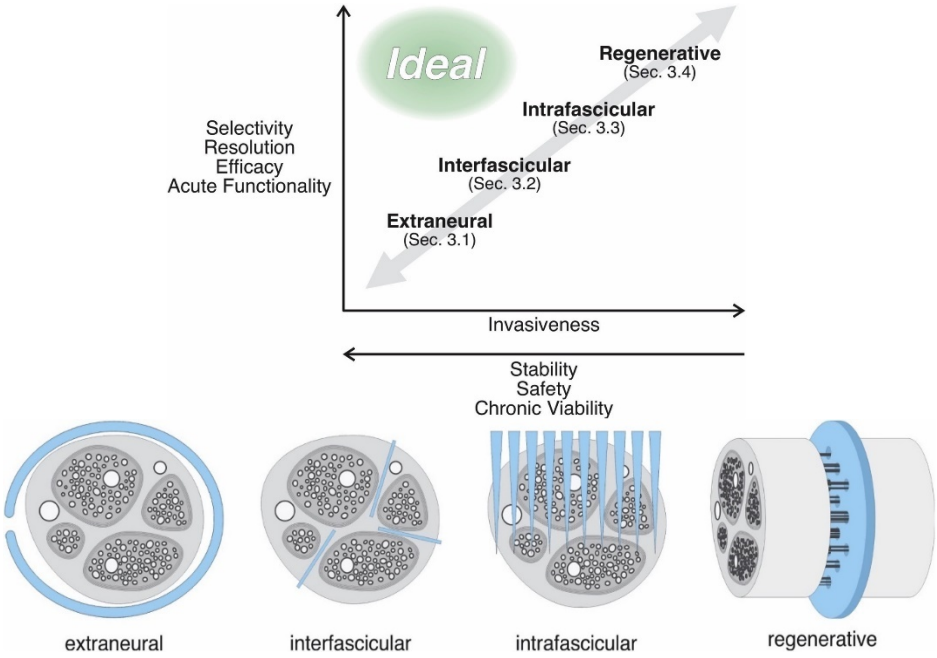

Figure 2.2. Illustration of the trade-off between invasiveness and selectivity of the existing PNI types (top row) and illustration of standard PNI designs (bottom row). Reprinted from Journal of Neuroscience Methods, Volume 332, Larson and Meng, A review for the peripheral nerve interface designer, Pages 108523, Copyright (2022), with permission from Elsevier.

- **Cuff Electrodes**

Extraneural interfaces are the most used PNI, with chronic implants being used for decades [39]. They consist of an insulating cylindrical sheath that wraps around the nerve with two or more contacts lying inside the sheath [40]. Recently, a study reported the safe use of chronic implants for over 3 to 7 years in four patients after transhumeral amputation [41]. The cuff electrode is one of the least invasive types of PNI, as the electrode surrounds the nerve's epineurium. This results in a straightforward surgical procedure, thereby minimising the risk of inducing neural tissue damage. Still, care must be taken to avoid constriction, which occurs when the electrode is fitted too tightly around the nerve trunk. Therefore, the cuff diameter should be big enough to accommodate swelling and avoid constriction [5]. In addition, axonal loss [42] and altered fascicular area [43] might also occur in long-term implants; yet, such alterations are gradually reversible to almost a normal level.

The signal recorded from cuff electrodes has a low amplitude, in the range of tens of μV, with most of its energy between 1 kHz and 3 kHz [44]. This signal is highly influenced by external sources of noise. For instance, the electromyographic signal is two to three orders of magnitude larger than the cuff signal [45]. As cuff electrodes

are positioned around the nerve, the resulting signal is the linear superposition of single fibre action potentials (SFAPs), with fascicles lying closer to the electrodes having a more substantial influence on the output than fibres lying on deeper sections of the nerve, leading to a poor spatial selectivity in the recordings [46]. Furthermore, as there is a linear relationship between the fibre diameter and nodal area, the signal amplitude is dependent on fibre diameter, with thicker fibres having a more significant weight on the overall signal recorded with cuff electrodes, resulting in a low functional selectivity [32].

Several electrode configurations have been suggested to enhance recordings with extraneural cuffs. The most classic example is the tripolar configuration, using three equally spaced electrodes, which has been shown to reduce electromyographic and other sources of electrical contamination [47]. The tripolar configuration was advanced by balancing the outer electrodes, further improving the electromyographic signal rejection [48].

- **FINE Electrodes**

The flat interface nerve electrode (FINE) was proposed to improve the spatial resolution of cuff electrodes. FINE has a rectangular shape that works by applying small forces to the nerve, consequently reshaping the nerve into a 'flattened oval' format. In doing so, the circumference of the nerve is increased, allowing fascicles to move closer to the surface, therefore decreasing the distance from the electrodes to the fascicles, and fascicles located in the middle of the nerve can be targeted more efficiently [49]. The chronic viability of FINE was assessed in cats, and the results showed that the electrode is functional and safe for opening heights of 1.3 mm and 0.5 mm at three months post-implantation [50].

2.2.3. INTRANEURAL INTERFACES

Intraneural interfaces penetrate the nerves' epineurium, resulting in closer proximity of the active electrodes to the axons. Intraneural interfaces are classified according to the position relative to the fascicles: The interfaces that only penetrate the epineurium are termed interfascicular, whereas the interfaces that penetrate the epineurium, perineurium, and endoneurium, are termed intrafascicular [51].

- **Interfascicular Interfaces**

Interfascicular interfaces penetrates the epineurium but not the fascicles. This way, superior access to the central axons is obtained compared to extraneural interfaces. The most traditional interfascicular interface is the slowly penetrating interfascicular nerve electrode (SPINE) [52]. In a study using cats, the authors reported no evidence of axon damage and no disruption to the perineurium; however, the experiments lasted 24 hours. The authors claimed this is insufficient time to obtain relevant histological evidence of nerve damage. Promising results were also obtained in rabbits, where a

fascicular selectivity of 0.98 was obtained [53]. To date, however, interfascicular interfaces have received less interest than extraneural and intrafascicular interfaces.

- **Intrafascicular Interfaces**

Intrafascicular interfaces penetrate all the nerve's protective layers; thus, direct contact with target fibres can be achieved. Two successful examples of intrafascicular interfaces are the longitudinal intrafascicular electrode (LIFE) [54], [55] and the transverse intrafascicular multichannel electrode (TIME) [56]. A study investigating the stimulation selectivity of an improved version of LIFE (thin-film longitudinal intrafascicular electrodes, tfLIFE) and TIME interfaces in pigs' forelimb muscles have shown a higher selectivity of the TIME [57]. This result is expected as TIME was designed to access a more significant subpopulation of fascicles than tfLIFE; therefore, the inability of the tfLIFE to sample the whole nerve likely resulted in the lower selectivity. Another study examining the selectivity of nerve fascicles with multipolar cuff, LIFE and TIME interfaces on the sciatic nerve of rats also reported a higher selectivity of TIME [58]. Further, as expected, the activation thresholds with intrafascicular electrodes were lower than with cuff electrodes (three to six times less than the thresholds for the intrafascicular interfaces).

The main disadvantages of intrafascicular interfaces are the increased risk of tissue damage and the need for specialised surgical skills for implantation. Nevertheless, the biocompatibility of intraneural interfaces is an emerging field with promising results. To name a few of the studies, Christensen et al. examined the safety of the Utah slant electrode array in the cat sciatic nerve in a chronic setting. The authors reported persistent inflammation that extended to 12 months, disruption of the blood-nerve barrier and a shift in fibre diameter towards smaller diameter fibres [59]. Another study investigating the biocompatibility of LIFE found a mild functional decline in the first month after implantation followed by recovery towards typical values in the following two months [60]. The TIME was also investigated for biocompatibility in a chronic setting of up to two months in the rat sciatic nerve. The results showed minimal axonal loss or demyelination [61]. Despite encouraging evidence, longevity with intraneural interfaces has not yet been performed at the same level as extraneural electrodes, so tissue reaction in a considerable period is unclear [46].

- **Regenerative Interfaces**

Regenerative interfaces are the most invasive electrode requiring transection of the nerve. They are designed so that nerve fibres can integrate with the interface. An example of a regenerative interface is the sieve electrode, consisting of a disk with many holes and contacts. The implantation procedure requires implanting the interface between two ends of the transected nerve. Then, the two ends of the nerve are sutured to the interface such that the nerve can regenerate through the sieve interface [40]. Regenerative interfaces are promising alternatives for single fibre selectivity, but further research is needed to address long-term safety [51]

2.3. SPATIAL AND FUNCTIONAL SELECTIVITY OF PNIS

A PNI would be maximally selective if it could stimulate and record from all individual neurons within a nerve. An example of a bidirectional control of an artificial neural prosthesis will be used to describe how this ideal system would work.

Control signals for a specific movement of the prosthesis can be obtained from motor fibres that originally innervated the missing limb muscle; hence, the selective control of all subsets of motor fibres contained within a nerve would allow for manipulating, independently, all specific muscles innervated by the same nerve [62]. Notably, the somatotopic organisation of peripheral nerves at the subfascicular level facilitate the selectivity of PNIs, since fascicular groups will innervate different targets and their organisation within a nerve remain bundled together for long distances [63]. Finally, sensory feedback can be provided to the user by recording tactile and force sensors and stimulating the individual afferent fibres [64]. The ultimate interface would allow a dexterous control of neuroprostheses and natural and selective sensory feedback.

Two categories of selectivity indexes exist to characterise PNIs. The first is topographical (or spatial) selectivity. It refers to the ability of an interface to record or stimulate a target population of nerve fibres that relates to an anatomical region (e.g., muscle, skin) supplied by a particular fascicle. An example of such application was a study using interfascicular electrodes, which reported high selectivity indexes of up to 0.98 (ranges from 0 to 1) by stimulating the tibial and peroneal fascicles within the sciatic nerve of rabbits [53]. Another study investigating the recording selectivity of TIME electrodes in the sciatic nerve of rats has shown that TIME can be used to selective record neural signals elicited by electrical stimulation from digital nerves innervating different areas of the rat's foot (toes 2 and 4) [65]

The second type of selectivity of PNIs is functional selectivity. Functional selectivity refers to the ability of an interface to stimulate or record only one specific fibre type that relates to the function conveyed by targeted axons [62]. Successful examples of functional selectivity obtained with PNIs include discrimination of different sensory modalities (proprioceptive, mechanical, and nociceptive) [66] and discrimination of neural signals based on conduction velocity [67].

2.4. INFORMATION EXTRACTION METHODS FOR EXTRANEURAL INTERFACES

The tripolar configuration has been traditionally used to record electroneurographic (ENG) signals with cuff electrodes. Despite the improvement in signal-to-noise ratio (SNR) over bipolar configurations [48], the energy contained in the signal is recorded with a single electrode, which limits the possibility of differentiating between afferent and efferent activity. Because of the small SNR, triggered averaging has been long-established to differentiate between the neural signal and external noise. Triggered

averaging works with the assumption that stochastic noise will be removed by recording the same stimulus multiple times and averaging the result. At the same time, the signal of interest will be enhanced. Despite improving the SNR, this technique requires enough time to compute the averages, making its use improper for real-time applications [11].

To estimate the contribution of distinct fibre types in compound action potential (CAP) recordings with a single tripole, a standard method is to calculate the expected latencies for each fibre group. By knowing the distance between the stimulating electrode and recording electrode and because of the proportional relationship of fibre diameter and conduction velocity, one can use features from the CAP such as initial slope [68] or rectified area [69] at the expected latencies to estimated fibre type contribution. However, with this approach, compound EMG volleys can contaminate the signal and generate 'bumps' in the signal, which may be misinterpreted as a neural signal [70].

The limitations of single-electrode recordings have led several groups to design multiple-contact electrodes so that spatial and temporal characteristics of the signal can be explored. For instance, researchers have shown through computer models and *in vivo* experiments that a single tetrapolar nerve cuff electrode could differentiate between afferent and efferent signals, with SNR levels comparable to the tripolar electrode [71].

A modelling study has shown how bioelectric source localisation methods, traditionally studied in EEG studies, may be used to identify neural pathways from multiple-electrode interfaces. Such information could be used for tracking, e.g., movement trajectories [72]. Later, the identification of pathways was investigated *in vivo* in the rat sciatic nerve. Using a matrix cuff of 56 contacts, the authors showed a mean success rate of 68.5% for single pathways and a 25.3% success rate for multiple pathways [73].

Beamforming algorithms, together with *a priori* knowledge of cuff geometry, have also been used to recover signals from individual fascicles with a FINE nerve cuff. Importantly, this method does not require knowing the location of the fascicles. The results in terms of spatial resolution suggested the possibility of functionally separating motor signals, and the lower complexity of the algorithm than the source localisation could be an advantage for real-time applications [74]. Since functional units of axons tend to be grouped within the same fascicle, distinguishing fascicular activity with extraneural cuffs would allow one to control prosthetic limbs with a high degree of freedom and the possibility to evoke robust natural sensations [75].

Another approach to discriminate bioelectric activity from peripheral nerves using multiple sensors integrates spatial and temporal information to construct templates for a given neural pathway [76]. In this case, a neural pathway is defined as a group of

nerve fibres responsible for a particular function. Then, in a training set, a spatiotemporal *fingerprint* is used to generate a tailored matched filter for a given pathway, used to classify different test scenarios. The spatiotemporal approach was compared with a Bayesian spatial filter (BSF) [77] and the velocity-selective recording method [78]. The results showed a better accuracy for the spatiotemporal method over the BSF and velocity-selective recording for all test scenarios and levels of the signal-to-noise ratio of the signal, as well as a smaller fraction of missed spikes.

The spatiotemporal approach was further validated in acute experiments using naturally evoked CAPs and four classification techniques: (i) matched filter, (ii) random forest, (iii) neural net, and (iv) random forest applied to signals pre-processed using rectified-bin-integration in different lengths of time-window. Similar to simulated data, the acute experiments indicated that the spatiotemporal approach could outperform BSF and velocity-selective recording approaches [79]. However, a sampling frequency of 30 kHz was used for both studies, which may affect the velocity-selective recording performance. In addition, the authors did not inform metrics of computational complexity, so the application in real-time may be limited. Finally, the supervised approach requires prior knowledge of the types of fibres and their fascicular location to train the classifier, perhaps limiting real-time applicability.

2.4.1. VELOCITY-SELECTIVE RECORDING

Taking advantage of the proportional relationship between fibre diameter and conduction velocity [80], researchers have proposed a method termed *velocity-selective recording* (VSR) to extract more information from nerve cuffs [81]. This method is based on using a *multiple-electrode cuff* (MEC) containing $N > 1$ linearly spaced tripoles. Therefore, as AP travel along the cuff, common waveforms appear at the N electrodes but with a time delay (T) equal to the quotient of the inter-electrode distance (d) and the propagation velocity (v) of the (compound) action potential [82].

$$T = {}^{d}/_{v}$$

Then, the N outputs are artificially delayed with a range of delay values (τ) with respect to a reference electrode (i.e., the delay between the first two channels will be τ, between the first and third channel will be 2τ, etc.), resulting in

$$V_D[n,\tau] = \sum_{i=1}^{C} V_{Ni}[n-(i-1)\tau]$$

where C is the number of recording channels (or electrodes) in the MEC and n is the sample index [83]. After summing all outputs N for a range of artificial delays τ, the output signals will add constructively when τ matches T. This procedure is named *delay-and-add,* and the resulting transformation can be considered a velocity-selective

filter. Notably, the principle works for both SFAPs and, because of linearity, CAPs [84].

The VSR method has two important properties for improving the ability to decode neural activity: (1) In the case of uncorrelated noise sources, there is an increase in the SNR of approximately $\sqrt{N}$ where N is the number of channels in the cuff, and (2) *afferent* and *efferent* activity can be distinguished by simply using positive or negative values of τ [82].

The VSR method has been experimentally demonstrated via electrically-evoked CAPs in the frog [84], [85], pig [83], [86] and earthworm [67]. The method has also been expanded for naturally occurring signals where respiration afferents could be extracted from the pig vagus nerve [83] and direct cutaneous stimulation through stroking of the L5 dermatome in a rat [87], [88].

2.5. LARGE ANIMAL MODELS VS SMALL ANIMAL MODELS

Animal models are essential during the pre-clinical phases of neural interfaces development. They are essential to assess the interface's acute and long-term properties, such as biocompatibility, stability, and selectivity. Currently, the rat is the most commonly used model for PNI investigation [5]. However, cats [50] and rabbits [53] have also been extensively used as animal models for PNI research. Recently, however, numerous studies have suggested that large animals may be more suitable models for the progress of PNIs and the investigation of the PNS. For instance, compared to rats, it has been shown that the pig cervical and subdiaphragmatic vagus nerve is more similar to the human in terms of nerve diameter and tissue type. The nerves of pigs and humans also have a polyfascicular structure, with the pig nerve having ten times more fascicles than humans. At the same time, rat nerves were generally monofascicular [14]. Another study compared the cervical and abdominal vagus nerve in mice, pigs, and humans has also reported a comparable diameter, polyfascicular structure, number of fibres, and amount of fibrous tissue between humans and porcine [15]. These differences have important implications for PNIs development, as the morphological parameters of the nerve influence electrical excitation thresholds [13].

The potential of the porcine peripheral nerve has also been studied for applications in nerve tissue engineering. A study characterising structural and extracellular matrix components of porcine peripheral nerves in the hind leg has demonstrated a higher similarity to humans than rodents in terms of anatomical, biochemical and cellular components [89]. Research into porcine's facial, ulnar, sural and laryngeal nerve has also suggested that the porcine model is a promising alternative for anatomic, topographical, histological and surgical characteristics [90].

The anatomical location and morphological characteristics of a nerve significantly influence the performance of PNIs. Additionally, the activation thresholds are highly dependent on the anatomical structures of a nerve, such as perineural thickness, fascicle diameter, the spatial distribution of fascicles, and axon diameter [13]. However, contrary to rodents, the detailed knowledge of the morphology and morphometry of porcine nerves is still limited. This information can be used to optimise stimulation strategies and new electrode designs and develop more realistic computational models of peripheral nerves.

CHAPTER 3. OUTLINE OF THE PHD WORK

The ulnar nerve is an important site for implanting PNIs to restore motor and sensory functions in upper limb prostheses [91]–[93]. The human UN has a polyfascicular structure, with the number of fascicles ranging from 8 fascicles in the elbow to 25 fascicles at the wrist [94]. In comparison, studies in rats have shown a monofascicular structure for proximal segments and a range of 1 - 4 fascicles for distal segments [17]. The difference in the fascicular number illustrates a critical gap between the peripheral nerve structure of small animal models and humans. Moreover, the small amplitudes and the noisy environment make it challenging to analyse and interpret the neural signal reliably. Alternative interfaces and signal processing algorithms were proposed to extract more information from neural cuffs. Still, different methodologies exist in the literature for other types of signals, such as the electromyographic. These options, which have not been evaluated for nerve recordings, need to be investigated and compared to the current methods for electroneurography data.

3.1. THESIS AIM

The thesis aimed to characterise the morphology and electrical excitability properties of the ulnar nerve in pigs and explore alternatives for improving functional selectivity recordings from multiple-electrode cuffs.

3.2. SPECIFIC RESEARCH QUESTIONS

Three studies were designed to address the thesis aim. They are described as follows:

Study I. Investigation of the morphometrical characteristics of the ulnar nerve in pigs

In humans, the number of fascicles in the ulnar nerve can range from approximately 5 to 35, depending on the region of the arm [94]. In rodents, however, the ulnar nerve has a monofascicular structure in proximal segments and can range from 1 to 4 fascicles in distal segments [17]. The discrepancy in the number of fascicles between rodents and humans is one of the several features that corroborate the need to improve animal models for PNI studies.

Study I, therefore, aimed to describe the ulnar nerve's morphology and morphometry in the distal forelimb of pigs and compare the results with humans and rodents to understand if the porcine has better translational characteristics for future use in PNI development and nerve regeneration studies.

Study I. Andreis, F.R., Metcalfe, B., Janjua, T. A. M., Fazan, V. P. S., Jensen, W., Meijs, S., Dos Santos Nielsen, T. G. N. Morphology and morphometry of the ulnar nerve in the forelimb of pigs. Muscle & Nerve (Submitted).

Study II. Characterisation of the excitability properties of the ulnar nerve

Several factors influence fibre response to electrical signals delivered through neural interfaces, such as nerve diameter, fascicular diameter, fascicular organisation, and fascicular number [13]. Many research groups have recently shown how the porcine nerve can serve as a superior translational model, better approximating human than rodent models [14], [15], [95]. Nevertheless, our knowledge of porcine nerves' excitation properties and neuroanatomy is limited, especially in somatic nerves.

Study II aimed to use the VSR technique to quantify the excitation properties of the ulnar nerve in pigs. A range of electrical stimulation parameters was used (amplitudes from 50 µA to 10 mA and pulse durations of 100 µs, 500 µs, 1000 µs, and 5000 µs) to stimulate the motor and the cutaneous branches of the ulnar nerve. The recording cuff, consisting of 14 rings, was used to differentiate fibre-activity based on the propagating velocity of the compound action potential.

Study II. Andreis, F.R., Metcalfe, B., Janjua, T. A. M., Jensen, W., Meijs, S., & Dos Santos Nielsen, T. G. N. The Use of the Velocity Selective Recording Technique to Reveal the Excitation Properties of the Ulnar Nerve in Pigs. Sensors, 22(1), [58]. https://doi.org/10.3390/s22010058.

Study III. Investigation of signal processing methods to improve the estimation of conduction velocity from multiple-electrode cuffs

To date, most neuromodulation and neuroprosthetic control methods use open-loop systems [5]. However, emerging methods, particularly the VSR technique, may be used for online discrimination of neural activity, as it is an unsupervised method that does not require *a priori* knowledge of the nerve morphology or training sets of data. In addition, because of the simplicity of the delay-and-add procedure, it could be implemented in a digital signal processor or a field-programmable gate array

Study III, therefore, aimed to explore different algorithms to extract information from multiple-electrode cuffs. The delay-and-add algorithm has been traditionally used for ENG; however, this is not the only technique available to determine propagating velocity in linear electrode arrays. Hence, we compared the performance of the delay-and-add with a maximum likelihood approach, initially designed for surface electromyography signals. In addition, variations of the maximum likelihood estimator and the delay-and-add were proposed and assessed.

Study III. Andreis, F.R., Metcalfe, B., Ribeiro, M., Janjua, T. A. M., Jensen, W., Meijs, S., Dos Santos Nielsen, T. G. N. A Comparison of Algorithms for Estimating Velocity-Selective Recording Using Multi-Electrode Cuffs (In preparation).

CHAPTER 4. METHODOLOGICAL APPROACHES

This chapter presents the methodological approaches for each of the thesis studies. All animal procedures were performed according to the Danish Veterinary and Food Administration under the Ministry of Food, Agriculture and Fisheries of Denmark (protocol number 2017-015-0201-0137).

4.1. ANIMAL PREPARATION

Nine female Danish Landrace pigs with a mean weight of 34.5 kg (range: 29.8 – 39.0 kg) were used. On arrival at the animal facility, the animals were given two weeks for acclimatisation at a room temperature of ≈ 24 °C with a 13:11 h light-dark cycle. At least two pigs were housed together to prevent social deprivation, and the animals fasted overnight before the surgery without water restriction.

4.1.1. SURGERY

The animals were intubated with a 1:1 oxygen and air mixture. A constant infusion of isotonic saline was administered through the jugular vein. The animals were placed in a supine position and anaesthetised with fentanyl (10 µg/hr/kg), propofol (2 mg/hr/kg) and sevoflurane (1.5 to 2.5 % minimum alveolar concentration). The depth of anaesthesia was verified via body temperature, end-tidal CO_2, heart rate, blood pressure, and tail reflex. Further, the animals were mechanically ventilated at 15 cycles per minute. The temperature was kept constant through a temperature-controlled air blanket (Mistral-Air Plus, MA1100, Amersfoort, The Netherlands) placed under the pig. Once the experiment was completed, the animals were euthanised by an overdose of pentobarbital.

An incision of approximately 20 cm was done on the right anterior forelimb to expose the ulnar nerve and the dorsal cutaneous branch of the ulnar nerve (DCBUN). Then, a segment of roughly 15 cm was freed from surrounding tissues.

4.2. ELECTRODES AND ELECTRONIC APPARATUSES

Three nerve cuffs were custom-made and developed with the technique described by Haugland [96]. Two stimulation cuffs were produced with three electrodes and mounted in a tripolar configuration; they were 10 mm long, with a centre-to-centre distance of 3 mm and an inner diameter of 1.8 mm. The tripolar configuration was used to connect a potentiometer between the end rings to balance the electrode impedances and reduce the stimulation artefact. Ideally, when the difference in

potential between the two outer electrodes is zero, no stimulus current flows past the recording electrode [97]. This procedure allowed to remove considerably the stimulation artefact, which without the presence of the potentiometer, completely obscured the compound action potential. Lastly, the two stimulation electrodes were connected to a general-purpose stimulus generator (STG4008, Multichannel Systems, Reutlingen, Germany).

The recording cuff, shown in Figure 4.1(a), was 50 mm long and contained 14 rings with a 3.5 mm inter-ring distance and an inner diameter of 2.6 mm. The width of the 12 centre rings was 0.5 mm, whereas the width of the outer electrodes was 1.0 mm. The end rings were short-circuited and used as a reference, and the animal was grounded through a subcutaneous stainless-steel needle coupled to the epidermis and the recording amplifier.

The recording cuff was connected to a custom-made preamplifier with an amplification of 10 and further to a computer-controlled amplifier (CyberAmp 380, Axon Instruments Inc., Burlingame, CA, USA). The gain of the amplifier was selected depending on the signal amplitude to avoid saturation. The mean overall voltage gain throughout the experiments was 75 dB (66 dB – 86 dB). The signals were then bandpass filtered with a high-pass filter at 100 Hz and a fourth-order Bessel low-pass filter with -3 dB frequency at 10 kHz. Finally, the signals were sampled at a 90 kSs^{-1} in a 16-bit resolution via a multifunction I/O device (PCIe-6363) and a rack-mounted BNC terminal (BNC-2090), both from National Instruments, Austin, TX, USA. An illustration of the experimental system is displayed in Figure 4.1(b).

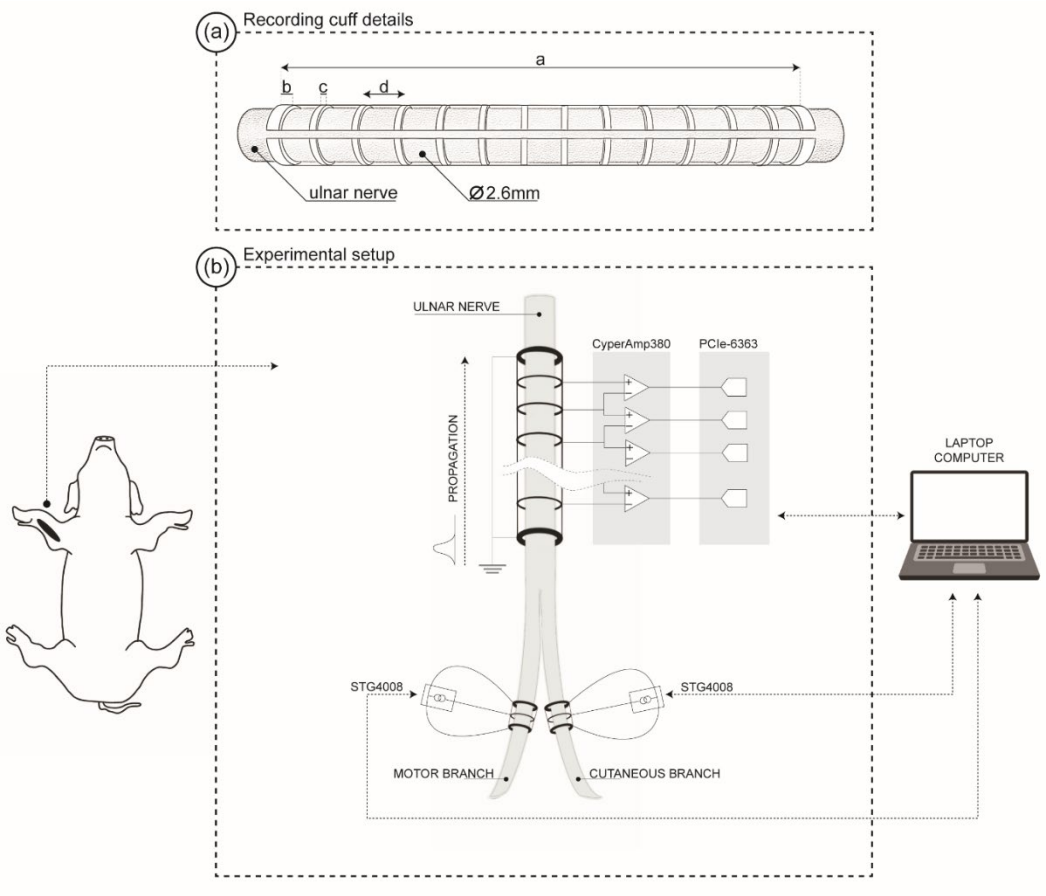

Figure 4.1. (a) Diagram of the 14 rings multiple-electrode cuff (MEC). The length of the MEC was 50 mm, with end rings (b) of 1 mm width and centre rings of 0.5 mm (c). The inter-electrode distance was 3.5 mm (d). The cuff had a diameter of 2.6 mm. (b) Experimental setup for recording the evoked compound action potentials by stimulation of the cutaneous and motor branch of the ulnar nerve—permission obtained from Andreis et al., Sensors; published by MDPI, 2022.

4.3. EXPERIMENTAL PROTOCOL

Trains of asymmetric rectangular charge-balanced biphasic pulses were produced with amplitudes ranging from 50 μA to 10 mA. The selected maximum amplitude was based on a pilot study that demonstrated that all fibres had been recruited at ten mA. Four levels of pulse duration were chosen: 100 μA, 500 μA, 1000 μA and 5000 μA. These values were chosen to investigate the threshold differences between different fibre types, which can be accentuated by decreasing the width of the cathodic phase of the stimulation [98]. The secondary phase of the stimulation waveform had an amplitude of 10% of the primary phase. The delay between each stimulus was 1 s with

a pseudo-random Gaussian interval with a maximum value of 250 ms. The purpose of a biphasic waveform was to reverse the electrochemical process that can arise at the electrode-tissue interface during the primary phase, reducing the risk of tissue damage [99]. Finally, the complete stimulation paradigm was repeated four times.

4.4. NEURAL SIGNAL PROCESSING

The raw data was segmented based on the stimulation onset using epochs from – 1 ms to 10 ms post-stimulus. As most of the ENG power spectrum lies between 1 – 3 kHz, the signal was bandpass filtered using an eighth order Butterworth filter with cut-off frequencies of 300 Hz and 8 kHz. Next, the bipolar signals were converted to tripolar by calculating the difference between pairs of adjacent channels and DC offsets were removed. The resulting compound action potentials were analysed with the delay-and-add algorithm (Section 2.4.1) [81]. The amplitude peaks and their respective velocities were extracted from the resulting intrinsic velocity spectrum. The peak threshold was defined as five times the baseline standard deviation. All signal processing was executed using MATLAB 2020a (Mathworks, MA, USA).

4.5. MORPHOLOGY AND MORPHOMETRY OF THE ULNAR NERVE

Seven Danish Landrace pigs with a mean weight of 34.1 kg (29.0 – 39.0 kg) were used for histological analysis. Three nerve segments of 2 mm were selected for each animal for the analysis. These nerve segments were extracted from (1) the main trunk of the ulnar nerve, roughly four cm proximally to the splitting point between the main trunk and the DCBUN, (2) at the main branch, approximately three cm distally to the splitting point, and (3) at the DCBUN, two cm distally to the splitting point.

The preparation of the nerves for histology consisted of fixation of the specimens by immersion in a 4% buffered formaldehyde solution and embedded in paraffin wax. The specimens were cut into 2.5 μm thick sections and stained with haematoxylin and eosin. The images were acquired with a digital slide scanner (NanoZoomer S360, Hamamatsu Photonics, Hamamatsu, Japan) at 40x magnification. The transverse sectional areas of the fascicles were obtained manually, and the number of fascicles was counted. Moreover, the external boundary of the epineurium was used to obtain the nerve area. The cross-sectional areas were transformed into effective diameters supposing a circular cross-section. The aforementioned structures were measured with the freehand selection tool from FIJI software [100].

A correction factor of 1.25 was applied to the nerve diameter, fascicle diameter and fibre diameter to account for tissue shrinkage due to embedding tissue in formalin. This factor was previously calculated by comparing frozen and formalin processed samples [101].

4.6. SIMULATION OF COMPOUND ACTION POTENTIALS

First, single myelinated fibre action potentials were generated following an inhomogeneous volume conductor model [102]. The transmembrane action potential function parameters were selected to produce a unipolar AP with a peak amplitude of 80 µV and a duration of 2 ms [87] (Figure 4.2).

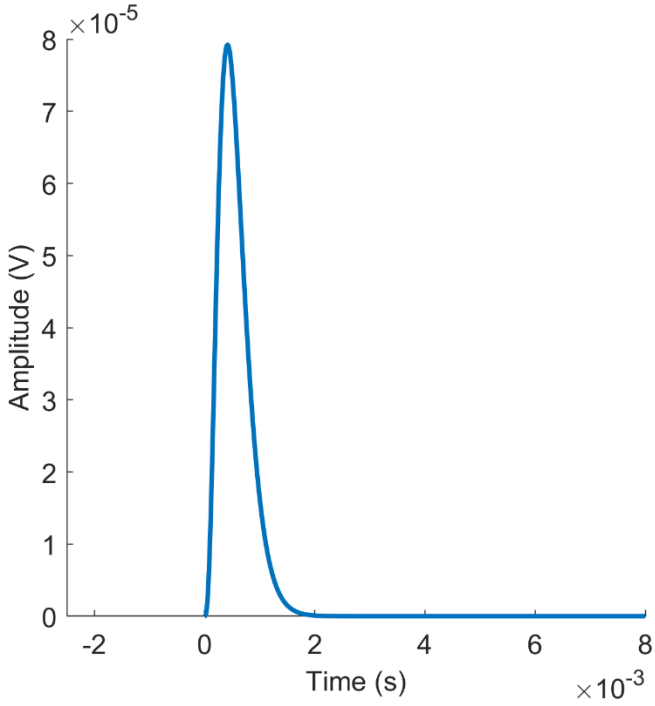

Figure 4.2. Resulting transmembrane action potential function with a peak amplitude of 80 µV and duration of 2 ms.

Multiple APs were added and delayed across the channels to generate the compound action potentials, resulting in a bimodal distribution with average conduction velocities of 16 ms^{-1} and 57 ms^{-1}. The artificial recording cuff contained 11 electrodes, connected bipolarly and equidistantly spaced by 3.5 mm.

CHAPTER 5. SUMMARY OF MAIN RESULTS

This chapter summarises the three studies defined in Chapter 3: Outline of PhD work.

5.1. SUMMARY OF STUDY I

Study I aimed at investigating the ulnar nerve's morphology and morphometry in the distal forelimb of pigs and compare these features with rodent and human data to analyse if the pig ulnar nerve may serve as a better translational animal model than rodents. To answer this question, seven Danish Landrace pigs with a mean weight of 34.1 kg were used for this study. Three nerve segments were extracted for histological analysis, located at:

1. the dorsal cutaneous branch of the ulnar nerve (DCBUN), 2 cm after separation from the UN.
2. The main trunk of the ulnar nerve (UN) at 4 cm before splitting into the DCBUN (proximal UN).
3. The main trunk of the UN at 3 cm after the splitting point (distal UN).

Three measures were obtained from the histological slides: i.e., nerve diameter, the number of fascicles and fascicle diameter.

The diameter of the nerve was significantly different across the three segments (p = 0.01), with the main trunk before splitting having the largest diameter ($p < 0.01$). The proximal main trunk also had the highest number of fascicles (median: 15, range: 14 – 16, $p < 0.01$) compared to the DCBUN (median: 11, range 6 – 13) and the distal UN (median: 10, range: 8 – 13). No difference was observed in the number of fascicles between the distal UN and the DCBUN (p = 0.97). Lastly, the fascicle diameter was also significantly different between the three nerve segments ($p < 0.01$), with the proximal UN having the largest mean fascicle diameter and the DCBUN the least.

The proximal branch of the UN had a mean diameter of 1713 µm, which is considerably larger than the 600 µm observed in rats [103] and more similar to the diameter of 2607 µm found in humans [94]. In the distal section of the UN, we observed a mean diameter of 1.39 mm, also larger than the 0.28 mm observed in rats [104] but still smaller than the diameter found in humans (2.82 mm) for a similarly located section [94].

At the main trunk, the median number of fascicles was 15, whereas, in Wistar rats, this number was between 1 and 4 [17]. In humans, however, the number of fascicles

at the forearm level was, on average, 20.7 [94]. The DCBUN showed a distinct pattern, wherein pigs, it was observed a median number of 11 fascicles, while human studies found five fascicles [105], [106].

These findings indicate that the pig's UN morphometry is likely a better model of the human UN than rodents. A closer resemblance between pig and human nerves is in accordance with studies investigating other nerves in pigs, such as the vagus nerve [14]. In this case, the authors found a comparable diameter between the pig and the human, while rats had diameters ten times smaller than humans. The authors also indicated that pigs had almost ten times more fascicles than the human vagus nerve [14].

5.2. SUMMARY OF STUDY II

Study II aimed to characterise the excitability properties of the ulnar nerve in pigs using velocity-selective recordings. A wide range of electrical stimulation parameters was applied to obtain the activation thresholds of the motor branch and the cutaneous branch of the ulnar nerve.

The results showed that the motor branch had only one predominant fibre type, with a mean conduction velocity of 63.64 ms^{-1}. The average current intensity needed to recruit 25% of the fibres when stimulating the motor branch was 629 µA, 593 µA, 571 µA or 560 µA for pulses duration of 100 µs, 500 µs, 1000 µs, and 5000 µs, respectively. There was a significant difference in the current intensity to activate 25% of the fibres for the different pulse durations ($p < 0.01$). The post-hoc analysis revealed that a higher current was needed for the 25% activation with a pulse duration of 100 µs. In contrast, between 500 µs, 1000 µs and 5000 µs, there was no statistically significant difference. In the case of the current needed to activate 75% of the fibres, the results showed that the threshold current was 3.5 mA, 3.7 mA, 3.6 mA, and 3.3 mA for pulse durations of 100 µs, 500 µs, 1000 µs, and 5000 µs, respectively. There was no difference in the current intensity between all levels of pulse width ($p = 0.45$).

Opposite to the motor branch, the cutaneous branch had two distinct fibre groups. The thickest fibre type had an average conduction velocity of 55.3 ms^{-1}, and the thinnest had a mean conduction velocity of 21.1 ms^{-1}. However, while the thickest fibre group was observed for all animals except one (that had contamination in the signal because of the stimulation artefact), the thinnest fibre group was observed only for three subjects.

The current intensity for recruitment of 25% of the fibres for the cutaneous branch was 625 µA, 544 µA, 544 µA and 583 µA for pulse durations of 100 µs, 500 µs, 1000 µs, and 5000 µs, respectively. Similar to the motor branch, there was a statistically significant difference ($p = 0.01$) between the current intensity across the different pulse widths. A higher current level was required for a pulse of 100 µs compared to

the other three levels. To recruit 75% of the fibres, the required current intensity was 3.6 mA for a pulse duration of 100 μs, 3.2 mA for a pulse duration of 500 μs, and 3.6 mA and 3.5 mA for pulse durations of 1000 μs and 5000 μs. In the same way as the motor branch, no significant difference was observed for the activation current across the four levels of pulse duration ($p = 0.06$).

These findings suggest the presence of two-fibre groups corresponding to Aβ and Aδ fibres in the cutaneous branch, although the slowest fibre group was only observed in three animals. For the motor branch, only Aβ fibres were present in the compound action potentials. A possible explanation for the detection of Aδ fibres in only three animals may be related to the amplifier's gain, which had to be adjusted to a level to avoid saturation of the stimulation artefact. This effect could be largely overcome by increasing the distance between the stimulation and recording electrodes by decreasing the number of channels in the recording cuff or decreasing the inter-electrode distance.

The non-significant differences in activation thresholds between pulses of 500 μs, 1000 μs, and 5000 μs indicate that the selected pulse durations lay on the horizontal asymptotic segment of the strength-duration curve [107]. Therefore, shorter pulse durations may be more appropriate to characterise the ulnar nerve excitation properties. Lastly, no C-fibres were observed, likely because of their small amplitude. A possible way to record C-fibres would be desheathing the epineurium, which has been shown to significantly increase the signal-to-noise ratio in extraneural recordings [108].

5.3. SUMMARY OF STUDY III

Study III compared several methods for estimating conduction velocity from multiple-electrode cuffs. Although the delay-and-add algorithm has been traditionally used for electroneurography, other research areas used different approaches to estimate conduction velocity from linear electrode arrays [109]. One example is the maximum likelihood estimator (MLE), which has gained success in electromyography research because of its high precision to estimate conduction velocity resulting in a standard deviation of fewer than 0.1 ms^{-1} [110]. Therefore, the MLE and VSR (delay-and-add) and variations of these algorithms were assessed with experimental and simulated data. The proposed variations were the fixed reference MLE (FR MLE) and modified VSR. Furthermore, the influence of the number of channels and SNR on precision and selectivity were measured.

For simulated data, the results showed that the precision of VSR and modified VSR is less influenced by the number of channels than the MLE and FR MLE, but only for high levels (i.e., 40 dB and 60 dB). For the selectivity analysis, all algorithms resulted in an increased selectivity with the addition of more channels in the electrode.

However, with less than seven channels, the higher selectivity of VSR and modified than the FR MLE and MLE is more pronounced.

The results from the experimental data demonstrated that the precision of all algorithms was significantly influenced by the number of channels in the recording cuff. For instance, the percent error when using four channels is 20.8% for the VSR and modified VSR, 13.5% for the MLE and 4.7% for FR MLE. When using nine channels, however, the modified VSR and VSR presented an error of 2.0%, whereas the MLE and FR MLE were 1.6% and 3.1%, respectively. The selectivity was also significantly influenced by the number of channels in the array, also stabilising at seven channels.

The most notable difference between the simulated and experimental data results was that for simulated data, an array with K channels always performed better or equal to an array with $K - 1$ channels. For some cases in the experimental data, adding a channel oppositely decreased the algorithm performance (e.g., VSR and modified VSR had the highest errors with four channels instead of the expected three). This difference highlights a significant limitation of these algorithms: the assumption of equal yet delayed waveforms propagating across the array. While this assumption holds true for simulated data, it is hardly the case for experimental data. Possible explanations have been proposed to explain the unequal shapes across the array, including uneven electrode-tissue impedance [86] or dispersion (i.e., axons belonging to a fibre type are not homogeneous in size and, consequently, conduction velocity). Therefore, dissimilar conduction velocities will attenuate and spread the waveforms over the length of the recording electrode) [69], [86].

CHAPTER 6. DISCUSSION

This thesis was motivated by the lack of existing information on the peripheral nervous system of large animal models. Therefore, this thesis aimed to provide novel information on the excitation properties and morphological characteristics of the ulnar nerve in pigs and, in addition, compare algorithms to decode ulnar nerve information from multiple-electrode cuffs. The studies provided summary values for the morphology of the ulnar nerve, indicating that it might be a suitable target for the advancement of peripheral nerve interfaces. The second study contributed to the understanding of the fibre populations contained within the ulnar nerve and what is the influence of stimulation parameters on the recruitment properties of the ulnar nerve. Finally, the third study investigated four algorithms and their ability to extract information from multiple-electrode cuffs. The effect of the number of channels and signal-to-noise ratio and their influence on precision and accuracy was also examined.

6.1. METHODOLOGICAL CONSIDERATIONS

6.1.1. CHOICE OF ANIMAL MODEL

Previous studies investigating the morphology of peripheral nerves in pigs have suggested that the median, radial, and ulnar nerves have equivalent sizes and multifascicular structures to humans [101], [111]. In particular, the ulnar nerve has the most superficial location of all nerves in the forelimb of pigs. It can be easily identified and accessed without accessing deeper structures [90], which is considered advantageous for assessing PNIs in acute and chronic settings because the superficial location may minimise the risks of surgically-induced damage. Still, it would be highly interesting to investigate the ulnar, radial, and medial nerves simultaneously since this would provide complete mapping of the forelimb nerves.

6.1.2. MORPHOMETRICAL ANALYSIS OF THE ULNAR NERVE

Immersion in formalin with paraffin embedding followed by haematoxylin and eosin (H&E) stain is one of the most common procedures for histological assessment of the PNS [112]. However, one of the main limitations of H&E is that the extracellular matrix is non-specifically stained, and the myelin sheath cannot be observed. Therefore, measures of the degree of myelination cannot be obtained [113]. The number of fibres and their size distribution were not presented in Study I since finding a reliable automatic method for axon size quantification has been difficult. A few algorithms were tested, and the results showed a significant amount of non-neural structures falsely identified as nerve fibres, especially for smaller fibres. It was observed that the false detection problem could be improved mainly by using a threshold diameter in these algorithms (i.e., fibres with a diameter less than the

threshold would not be counted). However, the result would be an underestimated number of fibres and an overestimation of the fibre size histograms. Still, the authors continue searching for ways of fibre quantification from the histological images of the UN. Finally, alternative procedures need to be performed for the morphometry of unmyelinated fibres. Successful examples include using a transmission electron microscope with lead citrate and uranyl acetate staining [106].

6.1.3. COMPOUND ACTION POTENTIAL RECORDINGS

One of the main challenges during the experiments was to reduce stimulation artefact contamination on the recorded signals. The short distance between the stimulation and recording cuff of approximately 2.5 cm resulted in significant artefacts, especially for longer pulse durations (i.e., 1000 μs and 5000 μs). The artefact was substantially reduced by balancing the impedances of the stimulation cuff, which allowed the recording of clear CAPs with almost negligible contamination. Alternatives would be simply increasing the distance between the stimulation and recording cuffs. However, this distance was limited by the length of the nerve. Still, shorter inter-electrode distances or fewer electrodes in the recording cuff could have increased the stimulation/recording distance and decreased artefact contamination. Another option to reduce the stimulation artefact contamination would be to connect a potentiometer to the end rings of the recording cuff, thereby balancing the difference in electrode impedance and linearising external signals within the cuff, reducing external contamination [48]. Interestingly, Study III shows that for the experimental data, seven channels would be sufficient for an optimised precision and selectivity. This shows how Study III could be used to guide optimisation of the electrode arrangement since, with the use of fewer electrodes (i.e., a larger distance between stimulation and recording interfaces), likely there would be less stimulation artefact contamination.

The idea of using a wide range of pulse durations was to investigate the thresholds for activation of different groups of fibres, as nerve fibres positioned at the same distance from the electrode have significantly higher threshold differences for shorter pulse widths [114]. Hence, the presence of a single fibre group when stimulating the motor branch and the presence of a secondary fibre group for the cutaneous branch for only three animals considerably limited the CAP analysis possibilities, both to characterise the excitability properties of the ulnar nerve to different pulse durations and to investigate the selectivity of the VSR method to multiple propagating velocities. For the cutaneous branch, where two fibre groups were observed in the CAPs for three animals, an improvement of the signal quality might have shown the slowest fibre group for more animals. This could be achieved, for example, by the removal of the epineurium [108]. Lastly, the choice of pulse durations likely resulted in a strength-duration curve limited to the horizontal asymptotic part of the curve. Therefore, shorter pulse widths are recommended for the investigation and optimisation of stimulation parameters.

Although this thesis assessed electrically evoked compound action potentials, which poses a limitation for the use of implantable neural interfaces, there have been a few studies demonstrating the usefulness of multiple-electrode cuffs to obtain information from naturally occurring (i.e., spontaneous) neural activity [83], [87], [115]. Improving the ability of multiple-electrode cuffs to decode spontaneous neural activity would be the natural pathway of progress that would allow its use in closed-loop neuromodulation systems and bidirectional bionic limbs.

6.1.4. METHODS FOR ESTIMATING CONDUCTION VELOCITY FROM MULTIPLE-ELECTRODE CUFFS

Study III investigated four algorithms to estimate conduction velocity from multiple-electrode cuffs for simulated and experimental CAPs. Although the algorithm's performance was similar for the two conditions, significant discrepancies were observed, mainly because the simulation method might be too simple to represent a realistic CAP propagating along the cuff. Improvements in the simulation algorithm could be made by considering:

(i) Unequal impedances across the electrodes result in disparate amplitudes between the channels.

(ii) Velocity dispersion, which will result in attenuation and spreading of the CAP as it propagates further from the stimulation electrode. The velocity dispersion effect could be included in simulated data by modelling the CAPs with a realistic nerve fibre distribution at a single location or even at multiple points since fibre distributions might change along the nerve [116], [117].

In addition to a better simulation model, algorithms based on broadband sensor array signal processing techniques could have been explored. More specifically, the space-time electrode array has outperformed the delay-and-add, especially for the selectivity of higher velocities [118].

6.2. IMPACT OF THE PHD WORK

- Study I showed that the UN in the forelimb of a pig bears a closer resemblance to the human analogue in terms of nerve diameter, fascicular number, and diameter. The large nerve diameter provides two main advantages over rodents: (i) human-size electrodes can be tested, and (ii) more space is available for assessing high-density multi-contact nerve cuffs. The second point is particularly important if combined with the polyfascicular structure of the porcine since even in studies using non-human primates, regions of monofascicular structures were reported for both the ulnar and median nerves. A monofascicular structure or even a smaller

number of fascicles can undoubtedly constrain the investigation of selective fascicle stimulation [119].

- Study II characterised the excitability properties of the UN. The results can be used to predict which current intensities are needed to recruit UN fibres. Moreover, the results indicate that the DCBUN contains two distinct fibre groups while the main trunk appears to have a single fibre group. Combined with the superficial location of the UN, this is an interesting feature that can be explored in, e.g., neuroscience research, where electrical stimulation is used to probe the CNS. Put in other words, if one wants to elicit sensations mediated by thinly myelinated Aδ fibres (pain, crude touch, temperature), one can opt for stimulating the DCBUN. In contrast, the main trunk contains only myelinated Aβ fibres, responsible mediating for touch and pressure. It has to be emphasised that C-fibres are likely present in these nerves; however, C-fibres require considerably larger stimulation amplitudes to be evoked (it can be as high as 45 times the threshold for A-fibres [108]).

- Study III investigated alternative ways of extracting information from multiple-electrode cuffs and can be used to assist researchers in designing an interface. By knowing the SNR of the signal, one can reasonably estimate how many channels are needed in the interface to achieve satisfactory precision and accuracy. For instance, with a PSNR of 60 dB, only three channels are needed to have sufficient precision and accuracy with the VSR method. However, with a PSNR of 20 dB, one would need six channels even to detect the velocity of a propagating signal.

6.3. CONCLUSIONS

Information on the somatic nervous system of large animals is still limited. However, a few existing studies, especially for the autonomic nervous system, have indicated that pigs have favourable characteristics and could be an improvement over rodents as a model for peripheral nerve interfaces development [14], [95]. The work in this thesis, in particular, Study I and Study II, have provided a characterisation of the ulnar nerve in the forelimb of pigs. In Study I, the morphology of the ulnar nerve was assessed, and the findings were compared to humans and rodents, indicating that the pig ulnar nerve can better approximate the human analogous. In Study II, the velocity-selective recording technique was used to reveal the ulnar nerve's excitation properties and underlying axonal distribution. Finally, Study III has used the experimental data, combined with a simulation approach, to investigate several algorithms for estimating conduction velocity from linear electrode arrays. The results provide precision and accuracy measures for a range of electrode numbers and SNR values.

LITERATURE LIST

[1] M. R. Van Balken, H. Vergunst, and B. L. H. Bemelmans, “The use of electrical devices for the treatment of bladder dysfunction: A review of methods,” *J. Urol.*, vol. 172, no. 3, pp. 846–851, 2004.

[2] H. H. O. Müller, S. Moeller, C. Lücke, A. P. Lam, N. Braun, and A. Philipsen, “Vagus nerve stimulation (VNS) and other augmentation strategies for therapy-resistant depression (TRD): Review of the evidence and clinical advice for use,” *Front. Neurosci.*, vol. 12, no. APR, pp. 1–10, 2018.

[3] A. Straube, J. Ellrich, O. Eren, B. Blum, and R. Ruscheweyh, “Treatment of chronic migraine with transcutaneous stimulation of the auricular branch of the vagal nerve (auricular t-VNS): a randomized, monocentric clinical trial,” *J. Headache Pain*, vol. 16, no. 1, 2015.

[4] J. del Valle and X. Navarro, “Interfaces with the Peripheral Nerve for the Control of Neuroprostheses,” in *International Review of Neurobiology*, 1st ed., vol. 109, Elsevier Inc., 2013, pp. 63–83.

[5] C. E. Larson and E. Meng, “A review for the peripheral nerve interface designer,” *J. Neurosci. Methods*, vol. 332, no. June 2019, p. 108523, 2020.

[6] S. Raspopovic, G. Valle, and F. M. Petrini, “Sensory feedback for limb prostheses in amputees,” *Nat. Mater.*, vol. 20, no. 7, pp. 925–939, 2021.

[7] P. D. Ganzer and G. Sharma, “Opportunities and challenges for developing closed-loop bioelectronic medicines,” *Neural Regen. Res.*, vol. 14, no. 1, pp. 46–50, 2019.

[8] M. Cracchiolo *et al.*, “Bioelectronic medicine for the autonomic nervous system: clinical applications and perspectives,” *J. Neural Eng.*, vol. 18, no. 4, Feb. 2021.

[9] L. Goudman *et al.*, “Cortical mapping of painful electrical stimulation by quantitative electroencephalography: Unraveling the time-frequency-channel domain,” *J. Pain Res.*, vol. 10, pp. 2675–2685, 2017.

[10] T. A. M. Janjua, T. G. N. dos S. Nielsen, F. R. Andreis, S. Meijs, and W. Jensen, “The effect of peripheral high-frequency electrical stimulation on the primary somatosensory cortex in pigs,” *IBRO Neurosci. Reports*, vol. 11, no. June, pp. 112–118, 2021.

[11] K. Yoshida, M. J. Bertram, T. G. Hunter Cox, and R. R. Riso, “Peripheral

Nerve Recording Electrodes and Techniques," in *Neuroprosthetics*, 2017, pp. 377–466.

[12] S. S. Sunderland, "The anatomy and physiology of nerve injury," *Muscle Nerve*, vol. 13, no. 9, pp. 771–784, 1990.

[13] Y. Grinberg, M. A. Schiefer, D. J. Tyler, and K. J. Gustafson, "Fascicular perineurium thickness, size, and position affect model predictions of neural excitation," *IEEE Trans. Neural Syst. Rehabil. Eng.*, vol. 16, no. 6, pp. 572–581, 2008.

[14] N. A. Pelot *et al.*, "Quantified Morphology of the Cervical and Subdiaphragmatic Vagus Nerves of Human, Pig, and Rat," *Front. Neurosci.*, vol. 14, no. November, pp. 1–19, Nov. 2020.

[15] N. Stakenborg *et al.*, "Comparison between the cervical and abdominal vagus nerves in mice, pigs, and humans," *Neurogastroenterol. Motil.*, vol. 32, no. 9, pp. 1–8, 2020.

[16] J. D. Stewart, "Peripheral nerve fascicles: Anatomy and clinical relevance," *Muscle and Nerve*, vol. 28, no. 5, pp. 525–541, 2003.

[17] A. P. Santos, C. A. Suaid, V. P. S. Fazan, and A. A. Barreira, "Microscopic anatomy of brachial plexus branches in wistar rats," *Anat. Rec.*, vol. 290, no. 5, pp. 477–485, 2007.

[18] D. U. Silverthorn, *Human Physiology: An Integrated Approach*, 6th ed. Pearson, 2013.

[19] A. J. Vander, J. Sherman, and D. S. Luciano, *Human Physiology: The Mechanisms of Body Function*, 8th ed. McGraw-Hill, 2001.

[20] E. R. Kandel, J. H. Schwartz, T. M. Jessel, S. A. Siegelbaum, and J. Hudspeth, A, Eds., *Principles of Neural Science*, 5th ed. McGraw-Hill, 2012.

[21] E. Marieb and S. Keller, *Essentials of Human Anatomy & Physiology*, 12th ed. Pearson, 2017.

[22] J. Erlanger, H. S. Gasser, and G. H. Bishop, "THE COMPOUND NATURE OF THE ACTION CURRENT OF NERVE AS DISCLOSED BY THE CATHODE RAY OSCILLOGRAPH," *Am. J. Physiol. Content*, vol. 70, no. 3, pp. 624–666, Nov. 1924.

[23] H. S. Gasser and J. Erlanger, "THE RÔLE PLAYED BY THE SIZES OF

THE CONSTITUENT FIBERS OF A NERVE TRUNK IN DETERMINING THE FORM OF ITS ACTION POTENTIAL WAVE," *Am. J. Physiol. Content*, vol. 80, no. 3, pp. 522–547, May 1927.

[24] R. Shane Tubbs, E. Rizk, M. M. Shoja, M. Loukas, N. Barbaro, and R. J. Spinner, Eds., *Nerves and nerve injuries*, Volume 1: Academic Press, 2015.

[25] N. M. Kane and A. Oware, "Nerve conduction and electromyography studies," *J. Neurol.*, vol. 259, no. 7, pp. 1502–1508, 2012.

[26] A. Mallik and A. I. Weir, "Nerve conduction studies: essentials and pitfalls in practice," *J. Neurol. Neurosurg. Psychiatry*, vol. 76, no. Suppl 2, pp. ii23–ii31, 2005.

[27] M. Tosato, K. Yoshida, E. Toft, V. Nekrasas, and J. J. Struijk, "Closed-loop control of the heart rate by electrical stimulation of the vagus nerve," *Med. Biol. Eng. Comput.*, vol. 44, no. 3, pp. 161–169, 2006.

[28] E. Brunton, C. W. Blau, and K. Nazarpour, "Separability of neural responses to standardised mechanical stimulation of limbs," *Sci. Rep.*, vol. 7, no. 1, pp. 1–14, 2017.

[29] W. T. Liberson, J. Holmquest, H, D. Scot, and M. Dow, "Functional electrotherapy: stimulation of the peroneal nerve synchronized with the swing phase of the gait of hemiplegic patients," *Arch Phys Med*, vol. 42, pp. 101–105, 1961.

[30] S. Alexander and D. Rowan, "Electrical control of urinary incontinence by radio implant. A report of 14 patients," *Br. J. Surg.*, vol. 55, no. 5, pp. 358–364, Dec. 1968.

[31] J. P. Judson and W. W. L. Glenn, "Radio-Frequency Electrophrenic Respiration," *JAMA*, vol. 203, no. 12, p. 1033, Mar. 1968.

[32] W. M. Grill, S. E. Norman, and R. V. Bellamkonda, "Implanted neural interfaces: Biochallenges and engineered solutions," *Annu. Rev. Biomed. Eng.*, vol. 11, pp. 1–24, 2009.

[33] M. Camilleri *et al.*, "Intra-abdominal vagal blocking (VBLOC therapy): Clinical results with a new implantable medical device," *Surgery*, vol. 143, no. 6, pp. 723–731, 2008.

[34] W. He *et al.*, "Transcutaneous auricular vagus nerve stimulation for pediatric epilepsy: Study protocol for a randomized controlled trial," *Trials*, vol. 16,

no. 1, pp. 1–6, 2015.

[35] A. J. Rush *et al.*, "Vagus nerve stimulation (VNS) for treatment-resistant depressions: A multicenter study," *Biol. Psychiatry*, vol. 47, no. 4, pp. 276–286, 2000.

[36] M. K. Haugland and T. Sinkjaer, "Cutaneous whole nerve recordings used for correction of footdrop in hemiplegic man," *IEEE Trans. Rehabil. Eng.*, vol. 3, no. 4, pp. 307–317, 1995.

[37] K. A. Yildiz, A. Y. Shin, and K. R. Kaufman, "Interfaces with the peripheral nervous system for the control of a neuroprosthetic limb: a review," *J. Neuroeng. Rehabil.*, vol. 17, no. 1, p. 43, Dec. 2020.

[38] K. S. Hong, N. Aziz, and U. Ghafoor, "Motor-commands decoding using peripheral nerve signals: A review," *J. Neural Eng.*, vol. 15, no. 3, 2018.

[39] K. Christian and G. E. Loeb, "Conduction studies in peripheral cat nerve using implanted electrodes: I. Methods and findings in controls," *Muscle Nerve*, vol. 11, no. 9, pp. 922–932, 1988.

[40] R. A. Coker, E. R. Zellmer, and D. W. Moran, "Micro-channel sieve electrode for concurrent bidirectional peripheral nerve interface. Part A: Recording," *J. Neural Eng.*, vol. 16, no. 2, 2019.

[41] M. Ortiz-Catalan, E. Mastinu, P. Sassu, O. Aszmann, and R. Brånemark, "Self-Contained Neuromusculoskeletal Arm Prostheses," *N. Engl. J. Med.*, vol. 382, no. 18, pp. 1732–1738, 2020.

[42] J. O. Larsen, M. Thomsen, M. Haugland, and T. Sinkjær, "Degeneration and regeneration in rabbit peripheral nerve with long-term nerve cuff electrode implant: A stereological study of myelinated and unmyelinated axons," *Acta Neuropathol.*, vol. 96, no. 4, pp. 365–378, 1998.

[43] W. Girsch *et al.*, "Histological assessment of nerve lesions caused by epineurial electrode application in rat sciatic nerve," *J. Neurosurg.*, vol. 74, no. 4, pp. 636–642, 1991.

[44] D. J. Tyler, "Electrodes for the Neural Interface," in *Neuromodulation*, 2nd Ed., Elsevier, 2018, pp. 239–274.

[45] J. K. Chapin and K. A. Moxon, Eds., *Neural Prostheses for Restoration of Sensory and Motor Function*, 1st ed. Boca Raton, FL: CRC Press, 2000.

[46] E. H. Rijnbeek, N. Eleveld, and W. Olthuis, “Update on peripheral nerve electrodes for closed-loop neuroprosthetics,” *Front. Neurosci.*, vol. 12, no. MAY, pp. 1–9, 2018.

[47] R. B. Stein, D. Charles, L. Davis, J. Jhamandas, A. Mannard, and T. R. Nichols, “Principles Underlying New Methods for Chronic Neural Recording,” *Can. J. Neurol. Sci. / J. Can. des Sci. Neurol.*, vol. 2, no. 3, pp. 235–244, 1975.

[48] J. J. Struijk and M. Thomsen, “Tripolar nerve cuff recording: Stimulus artifact, EMG, and the recorded nerve signal,” *Annu. Int. Conf. IEEE Eng. Med. Biol. - Proc.*, vol. 17, no. 2, pp. 1105–1106, 1995.

[49] D. J. Tyler and D. M. Durand, “Functionally selective peripheral nerve stimulation with a flat interface nerve electrode,” *IEEE Trans. Neural Syst. Rehabil. Eng.*, vol. 10, no. 4, pp. 294–303, Dec. 2002.

[50] D. K. Leventhal, M. Cohen, and D. M. Durand, “Chronic histological effects of the flat interface nerve electrode,” *J. Neural Eng.*, vol. 3, no. 2, pp. 102–113, 2006.

[51] V. Paggi, O. Akouissi, S. Micera, and S. P. Lacour, “Compliant peripheral nerve interfaces,” *J. Neural Eng.*, vol. 18, no. 3, p. 031001, Jun. 2021.

[52] D. J. Tyler and D. M. Durand, “A slowly penetrating interfascicular nerve electrode for selective activation of peripheral nerves,” *IEEE Trans. Rehabil. Eng.*, vol. 5, no. 1, pp. 51–61, 1997.

[53] T. N. Nielsen, C. Sevcencu, and J. J. Struijk, “Fascicle-selectivity of an intraneural stimulation electrode in the rabbit sciatic nerve,” *IEEE Trans. Biomed. Eng.*, vol. 59, no. 1, pp. 192–197, 2012.

[54] K. Yoshida and K. Horch, “Selective Stimulation of Peripheral Nerve Fibers using Dual Intrafascicular Electrodes,” *IEEE Trans. Biomed. Eng.*, vol. 40, no. 5, pp. 492–494, 1993.

[55] P. H. Veltink, J. A. van Alsté, and H. B. K. Boom, “Multielectrode intrafascicular and extraneural stimulation,” *Med. Biol. Eng. Comput.*, vol. 27, no. 1, pp. 19–24, Jan. 1989.

[56] T. Boretius *et al.*, “A transverse intrafascicular multichannel electrode (TIME) to interface with the peripheral nerve,” *Biosens. Bioelectron.*, vol. 26, no. 1, pp. 62–69, 2010.

[57] A. Kundu, K. R. Harreby, K. Yoshida, T. Boretius, T. Stieglitz, and W. Jensen, “Stimulation selectivity of the ‘thin-film longitudinal intrafascicular electrode’ (tfLIFE) and the ‘transverse intrafascicular multi-channel electrode’ (time) in the large nerve animal model,” *IEEE Trans. Neural Syst. Rehabil. Eng.*, vol. 22, no. 2, pp. 400–410, 2014.

[58] J. Badia, T. Boretius, D. Andreu, C. Azevedo-Coste, T. Stieglitz, and X. Navarro, “Comparative analysis of transverse intrafascicular multichannel, longitudinal intrafascicular and multipolar cuff electrodes for the selective stimulation of nerve fascicles,” *J. Neural Eng.*, vol. 8, no. 3, 2011.

[59] M. B. Christensen, S. M. Pearce, N. M. Ledbetter, D. J. Warren, G. A. Clark, and P. A. Tresco, “The foreign body response to the Utah Slant Electrode Array in the cat sciatic nerve,” *Acta Biomater.*, vol. 10, no. 11, pp. 4650–4660, 2014.

[60] N. Lago, K. Yoshida, K. P. Koch, and X. Navarro, “Assessment of biocompatibility of chronically implanted polyimide and platinum intrafascicular electrodes,” *IEEE Trans. Biomed. Eng.*, vol. 54, no. 2, pp. 281–290, 2007.

[61] J. Badia, T. Boretius, A. Pascual-Font, E. Udina, T. Stieglitz, and X. Navarro, “Biocompatibility of chronically implanted transverse intrafascicular multichannel electrode (TIME) in the rat sciatic nerve,” *IEEE Trans. Biomed. Eng.*, vol. 58, no. 8, pp. 2324–2332, 2011.

[62] S. Micera *et al.*, “On the use of longitudinal intrafascicular peripheral interfaces for the control of cybernetic hand prostheses in amputees,” *IEEE Trans. Neural Syst. Rehabil. Eng.*, vol. 16, no. 5, pp. 453–472, 2008.

[63] M. G. Honig, P. A. Frase, and S. J. Camilli, “The spatial relationships among cutaneous, muscle sensory and motoneuron axone during development of the chick hindlimb,” *Development*, vol. 125, no. 6, pp. 995–1004, 1998.

[64] R. R. Riso, “Strategies for providing upper extremity amputees with tactile and hand position feedback - Moving closer to the bionic arm,” *Technol. Heal. Care*, vol. 7, no. 6, pp. 401–409, 1999.

[65] J. Badia, S. Raspopovic, J. Carpaneto, S. Micera, and X. Navarro, “Spatial and functional selectivity of peripheral nerve signal recording with the transversal intrafascicular multichannel electrode (TIME),” *IEEE Trans. Neural Syst. Rehabil. Eng.*, vol. 24, no. 1, pp. 20–27, 2016.

[66] S. Raspopovic, J. Carpaneto, E. Udina, X. Navarro, and S. Micera, “On the

identification of sensory information from mixed nerves by using single-channel cuff electrodes," *J. Neuroeng. Rehabil.*, vol. 7, no. 1, pp. 1–15, 2010.

[67] K. Yoshida, G. A. M. Kurstjens, and K. Hennings, "Experimental validation of the nerve conduction velocity selective recording technique using a multi-contact cuff electrode," *Med. Eng. Phys.*, vol. 31, no. 10, pp. 1261–1270, 2009.

[68] S. C. M. A. Ordelman, L. Kornet, R. Cornelussen, H. P. J. Buschman, and P. H. Veltink, "An indirect component in the evoked compound action potential of the vagal nerve," *J. Neural Eng.*, vol. 7, no. 6, 2010.

[69] M. A. Castoro *et al.*, "Excitation properties of the right cervical vagus nerve in adult dogs," *Exp. Neurol.*, vol. 227, no. 1, pp. 62–68, 2011.

[70] M. K. Haugland and J. A. Hoffer, "Artifact-Free Sensory Nerve Signals Obtained from Cuff Electrodes During Functional Electrical Stimulation of Nearby Muscles," *IEEE Trans. Rehabil. Eng.*, vol. 2, no. 1, pp. 37–40, 1994.

[71] P. Sabetian and P. B. Yoo, "Feasibility of differentially measuring afferent and efferent neural activity with a single nerve cuff electrode," *J. Neural Eng.*, vol. 17, no. 1, p. 016040, Jan. 2020.

[72] J. Zariffa and M. R. Popovic, "Solution space reduction in the peripheral nerve source localization problem using forward field similarities," *J. Neural Eng.*, vol. 5, no. 2, pp. 191–202, 2008.

[73] J. Zariffa, M. K. Nagai, M. Schuettler, T. Stieglitz, Z. J. Daskalakis, and M. R. Popovic, "Use of an experimentally derived leadfield in the peripheral nerve pathway discrimination problem," *IEEE Trans. Neural Syst. Rehabil. Eng.*, vol. 19, no. 2, pp. 147–156, 2011.

[74] B. Wodlinger and D. M. Durand, "Localization and recovery of peripheral neural sources with beamforming algorithms," *IEEE Trans. Neural Syst. Rehabil. Eng.*, vol. 17, no. 5, pp. 461–468, 2009.

[75] B. Wodlinger and D. M. Durand, "Selective recovery of fascicular activity in peripheral nerves," *J. Neural Eng.*, vol. 8, no. 5, 2011.

[76] R. G. L. Koh, A. I. Nachman, and J. Zariffa, "Use of spatiotemporal templates for pathway discrimination in peripheral nerve recordings: A simulation study," *J. Neural Eng.*, vol. 14, no. 1, 2017.

[77] Y. Tang, B. Wodlinger, and D. M. Durand, "Bayesian spatial filters for source

signal extraction: A study in the peripheral nerve," *IEEE Trans. Neural Syst. Rehabil. Eng.*, vol. 22, no. 2, pp. 302–311, 2014.

[78] J. Taylor, M. Schuettler, C. Clarke, and N. Donaldson, "A summary of the theory of velocity selective neural recording," *Proc. Annu. Int. Conf. IEEE Eng. Med. Biol. Soc. EMBS*, pp. 4649–4652, 2011.

[79] R. G. L. Koh, A. I. Nachman, and J. J. J. Zariffa, "Classification of naturally evoked compound action potentials in peripheral nerve spatiotemporal recordings," *Sci. Rep.*, vol. 9, no. 1, pp. 1–13, 2019.

[80] W. A. H. Rushton, "A theory of the effects of fibre size in medullated nerve," *J. Physiol.*, vol. 115, no. 1, pp. 101–122, 1951.

[81] J. T. Taylor, N. Donaldson, and J. Winter, "Multiple-electrode nerve cuffs for low-velocity and velocity-selective neural recording," *Med. Biol. Eng. Comput.*, vol. 42, no. 5, pp. 634–643, Sep. 2004.

[82] N. Donaldson, R. Rieger, M. Schuettler, and J. Taylor, "Noise and selectivity of velocity-selective multi-electrode nerve cuffs," *Med. Biol. Eng. Comput.*, vol. 46, no. 10, pp. 1005–1018, 2008.

[83] B. W. Metcalfe, T. N. Nielsen, N. de N. Donaldson, A. J. Hunter, and J. T. Taylor, "First demonstration of velocity selective recording from the pig vagus using a nerve cuff shows respiration afferents," *Biomed. Eng. Lett.*, vol. 8, no. 1, pp. 127–136, 2018.

[84] R. Rieger *et al.*, "Experimental determination of compound action potential direction and propagation velocity from multi-electrode nerve cuffs," *Med. Eng. Phys.*, vol. 26, no. 6, pp. 531–534, 2004.

[85] M. Schuettler, N. Donaldson, V. Seetohul, and J. Taylor, "Fibre-selective recording from the peripheral nerves of frogs using a multi-electrode cuff," *J. Neural Eng.*, vol. 10, no. 3, 2013.

[86] B. Metcalfe, T. Nielsen, and J. Taylor, "Velocity Selective Recording: A Demonstration of Effectiveness on the Vagus Nerve in Pig," *Proc. Annu. Int. Conf. IEEE Eng. Med. Biol. Soc. EMBS*, vol. 2018-July, pp. 2945–2948, 2018.

[87] B. W. Metcalfe, A. J. Hunter, J. E. Graham-Harper-Cater, and J. T. Taylor, "Array processing of neural signals recorded from the peripheral nervous system for the classification of action potentials," *J. Neurosci. Methods*, vol. 347, no. October 2020, p. 108967, 2021.

[88] B. Metcalfe, D. Chew, C. Clarke, N. Donaldson, and J. Taylor, "Fibre-selective discrimination of physiological ENG using velocity selective recording: Report on pilot rat experiments," *2014 36th Annu. Int. Conf. IEEE Eng. Med. Biol. Soc. EMBC 2014*, no. August, pp. 2645–2648, 2014.

[89] L. Zilic, P. E. Garner, T. Yu, S. Roman, J. W. Haycock, and S. P. Wilshaw, "An anatomical study of porcine peripheral nerve and its potential use in nerve tissue engineering," *J. Anat.*, vol. 227, no. 3, pp. 302–314, 2015.

[90] T. Scholz, M. Pharaon, and G. R. D. Evans, "Peripheral nerve anatomy for regeneration studies in pigs: Feasibility of large animal models," *Ann. Plast. Surg.*, vol. 65, no. 1, pp. 43–47, 2010.

[91] S. Raspopovic *et al.*, "Bioengineering: Restoring natural sensory feedback in real-time bidirectional hand prostheses," *Sci. Transl. Med.*, vol. 6, no. 222, 2014.

[92] P. M. Rossini *et al.*, "Double nerve intraneural interface implant on a human amputee for robotic hand control," *Clin. Neurophysiol.*, vol. 121, no. 5, pp. 777–783, 2010.

[93] D. W. Tan, M. A. Schiefer, M. W. Keith, J. R. Anderson, J. Tyler, and D. J. Tyler, "A neural interface provides long-term stable natural touch perception," *Sci. Transl. Med.*, vol. 6, no. 257, pp. 1–11, Oct. 2014.

[94] N. A. Brill and D. J. Tyler, "Quantification of human upper extremity nerves and fascicular anatomy," *Muscle and Nerve*, vol. 56, no. 3, pp. 463–471, 2017.

[95] M. L. Settell *et al.*, "Functional vagotopy in the cervical vagus nerve of the domestic pig: Implications for the study of vagus nerve stimulation," *J. Neural Eng.*, vol. 17, no. 2, 2020.

[96] M. Haugland, "A flexible method for fabrication of nerve cuff electrodes," in *18th Annual International Conference of the IEEE Engineering and Medicine and Biology Society*, 1996, pp. 359–360.

[97] D. M. Woodbury and J. W. Woodbury, "Effects of Vagal Stimulation on Experimentally Induced Seizures in Rats," *Epilepsia*, vol. 31, pp. S7–S19, 1990.

[98] P. H. Gorman and J. T. Mortimer, "The Effect of Stimulus Parameters on the Recruitment Characteristics of Direct Nerve Stimulation," *IEEE Trans. Biomed. Eng.*, vol. BME-30, no. 7, pp. 407–414, 1983.

[99] P. H. Peckham and J. S. Knutson, "Functional Electrical Stimulation for Neuromuscular Applications," *Annu. Rev. Biomed. Eng.*, vol. 7, no. 1, pp. 327–360, 2005.

[100] J. Schindelin *et al.*, "Fiji: an open-source platform for biological-image analysis," *Nat. Methods*, vol. 9, no. 7, pp. 676–682, Jul. 2012.

[101] A. Kundu, K. R. Harreby, and W. Jensen, "Comparison of median and ulnar nerve morphology of Danish landrace pigs and Göttingen mini pigs," *Annu. Conf. ...*, pp. 1–4, 2012.

[102] J. J. Struijk, "The extracellular potential of a myelinated nerve fiber in an unbounded medium and in nerve cuff models," *Biophys. J.*, vol. 72, no. 6, pp. 2457–2469, 1997.

[103] J. A. Bertelli, M. Taleb, A. Saadi, J. -C Mira, and M. Pecot-Dechavassine, "The rat brachial plexus and its terminal branches: An experimental model for the study of peripheral nerve regeneration," *Microsurgery*, vol. 16, no. 2, pp. 77–85, 1995.

[104] M. J. Barton, J. Stjohn, A. Tatian, J. D. Riches, O. Mograby, and D. Mahns, "Morphological and morphometric analysis of the distal branches of the rat brachial plexus," *Ital. J. Anat. Embryol.*, vol. 121, no. 3, pp. 240–252, 2016.

[105] T. D. Luo *et al.*, "Transfer of the Dorsal Cutaneous Branch of the Ulnar Nerve for Restoration of Median Nerve Sensation: A Cadaveric Study," *Clin. Anat.*, vol. 31, no. 7, pp. 1006–1012, 2018.

[106] A. L. C. R. D. Oliveira, V. P. S. Fazan, W. Marques, and A. A. Barreira, "Dorsal cutaneous branch of the ulnar nerve: A light and electron microscopy histometric study," *J. Peripher. Nerv. Syst.*, vol. 16, no. 2, pp. 98–101, 2011.

[107] L. A. Geddes, "Accuracy Limitations of Chronaxie Values," *IEEE Trans. Biomed. Eng.*, vol. 51, no. 1, pp. 176–181, 2004.

[108] P. B. Yoo, N. B. Lubock, J. G. Hincapie, S. B. Ruble, J. J. Hamann, and W. M. Grill, "High-resolution measurement of electrically-evoked vagus nerve activity in the anesthetized dog," *J. Neural Eng.*, vol. 10, no. 2, 2013.

[109] R. Merletti, D. Farina, and M. Gazzoni, "The linear electrode array: A useful tool with many applications," *J. Electromyogr. Kinesiol.*, vol. 13, no. 1, pp. 37–47, 2003.

[110] D. Farina, W. Muhammad, E. Fortunato, O. Meste, R. Merletti, and H. Rix,

"Estimation of single motor unit conduction velocity from surface electromyogram signals detected with linear electrode arrays," *Med. Biol. Eng. Comput.*, vol. 39, no. 2000, pp. 225–236, Mar. 2001.

[111] R. R. Riso, A. Dalmose, M. Schuettler, and T. Stieglitz, "Activation of Muscles in the Pig Forelimb Using a Large Diameter Multipolar Nerve Cuff Installed on the Radial Nerve in the Axilla," *Proc. 5th Annu. Conf. Int. Funct. Electr. Stimul. Soc.*, no. September 2015, pp. 272–275, 2000.

[112] I. D. Pardo *et al.*, "Atlas of Normal Microanatomy, Procedural and Processing Artifacts, Common Background Findings, and Neurotoxic Lesions in the Peripheral Nervous System of Laboratory Animals," *Toxicol. Pathol.*, vol. 48, no. 1, pp. 105–131, 2020.

[113] V. Carriel, I. Garzón, M. Alaminos, and M. Cornelissen, "Histological assessment in peripheral nerve tissue engineering," *Neural Regen. Res.*, vol. 9, no. 18, pp. 1657–1660, 2014.

[114] W. M. Grill and J. T. Mortimer, "Stimulus waveforms for selective neural stimulation," *IEEE Eng. Med. Biol. Mag.*, vol. 14, no. 4, pp. 375–385, 1995.

[115] B. Metcalfe, D. Chew, C. Clarke, N. Donaldson, and J. Taylor, "An enhancement to velocity selective discrimination of neural recordings: Extraction of neuronal firing rates," *2014 36th Annu. Int. Conf. IEEE Eng. Med. Biol. Soc. EMBC 2014*, no. July 2015, pp. 4111–4114, 2014.

[116] F. Pehlivan, N. Dalkilic, and E. Kiziltan, "Does the conduction velocity distribution change along the nerve?," *Med. Eng. Phys.*, vol. 26, no. 5, pp. 395–401, 2004.

[117] R. S. Wijesinghe, F. L. H. Gielen, and J. P. Wikswo, "A model for compound action potentials and currents in a nerve bundle III: A comparison of the conduction velocity distributions calculated from compound action currents and potentials," *Ann. Biomed. Eng.*, vol. 19, no. 1, pp. 97–121, 1991.

[118] F. Karimi and S. R. Seydnejad, "Velocity Selective Neural Signal Recording Using a Space-Time Electrode Array," *IEEE Trans. Neural Syst. Rehabil. Eng.*, vol. 23, no. 5, pp. 837–848, Sep. 2015.

[119] N. Brill, K. Polasek, E. Oby, C. Ethier, L. Miller, and D. Tyler, "Nerve cuff stimulation and the effect of fascicular organization for hand grasp in nonhuman primates," *Proc. 31st Annu. Int. Conf. IEEE Eng. Med. Biol. Soc. Eng. Futur. Biomed. EMBC 2009*, pp. 1557–1560, 2009.

Appendix A. Permission for figure replication

Permission for Figure 2.1.

ELSEVIER LICENSE
TERMS AND CONDITIONS

Feb 15, 2022

This Agreement between Mr. Felipe Rettore Andreis ("You") and Elsevier ("Elsevier") consists of your license details and the terms and conditions provided by Elsevier and Copyright Clearance Center.

License Number	5250130998385
License date	Feb 15, 2022
Licensed Content Publisher	Elsevier
Licensed Content Publication	Journal of Orthopaedics
Licensed Content Title	Tobacco use and neurogenesis: A theoretical review of pathophysiological mechanism affecting the outcome of peripheral nerve regeneration
Licensed Content Author	Francisco Rodriguez-Fontan,Bradley Reeves,Krystle Tuaño,Salih Colakoglu,Laura D' Agostino,Rodrigo Banegas
Licensed Content Date	November–December 2020
Licensed Content Volume	22
Licensed Content Issue	n/a
Licensed Content Pages	5
Start Page	59

Permission for Figure 2.2.

ELSEVIER LICENSE
TERMS AND CONDITIONS

Feb 15, 2022

This Agreement between Mr. Felipe Rettore Andreis ("You") and Elsevier ("Elsevier") consists of your license details and the terms and conditions provided by Elsevier and Copyright Clearance Center.

License Number	5250220864945
License date	Feb 15, 2022
Licensed Content Publisher	Elsevier
Licensed Content Publication	Journal of Neuroscience Methods
Licensed Content Title	A review for the peripheral nerve interface designer
Licensed Content Author	Christopher E. Larson,Ellis Meng
Licensed Content Date	Feb 15, 2020
Licensed Content Volume	332
Licensed Content Issue	n/a
Licensed Content Pages	1
Start Page	108523
End Page	0
Type of Use	reuse in a thesis/dissertation

ISSN (online): 2246-1302
ISBN (online): 978-87-7573-916-5

AALBORG UNIVERSITY PRESS